Exploring the therapeutic mechanism of Yuebi decoction on nephrotic syndrome based on network pharmacology and experimental study

Tianwen Yao[1], Qingliang Wang[2], Shisheng Han[1], Yanqiu Xu[1], Min Chen[1], Yi Wang[1]

[1]Department of Nephrology, Yueyang Hospital of Integrated Traditional Chinese and Western Medicine, Shanghai University of Traditional Chinese Medicine, Shanghai 200437, China
[2]Shanghai Jing'an District Hospital of Traditional Chinese Medicine, Shanghai 200072, China

Correspondence to: Yi Wang; **email:** wangyi@shyueyanghospital.com
Keywords: Yuebi decoction, nephrotic syndrome, podocyte injury, network pharmacology, molecular docking
Received: January 17, 2024 **Accepted:** September 2, 2024 **Published:** September 20, 2024

ABSTRACT

Objective: This study aimed to explore the material basis of YBD and its possible mechanisms against NS through network pharmacology, molecular docking, and *in vivo* experiment.

Methods: Active ingredients and potential targets of YBD were obtained through TCMSP and SwissTargetPrediction. NS-related targets were obtained from GeneCards, PharmGKB, and OMIM databases. The herb-ingredient-target network and PPI network were constructed by Cytoscape 3.9.1 and STRING database. GO and KEGG analyses were performed by DAVID database and ClueGO plugin. The connection between main active ingredients and core targets were revealed by molecular docking. To ascertain the effects and molecular mechanisms of YBD, a rat model was established by PAN.

Results: We collected 124 active ingredients, 269 drug targets, and 2089 disease targets. 119 overlapping were screened for subsequent analysis. PPI showed that AKT1, STAT3, TRPC6, CASP3, JUN, PPP3CA, IL6, PTGS2, VEGFA, and NFATC3 were potential therapeutic targets of YBD against NS. Through GO and KEGG analyses, it showed the therapeutic effect of YBD on NS was closely involved in the regulation of pathways related to podocyte injury, including AGE-RAGE signaling pathway in diabetic complications and MAPK signaling pathway. Five key bioactive ingredients of YBD had the good affinity with the core targets. the experiment confirmed the renoprotective effects of YBD through reducing podocyte injury. Furthermore, YBD could downregulate expressions of PPP3CA, STAT3, NFATC3, TRPC6, and AKT1 in rats.

Conclusions: YBD might be a potential drug in the treatment of NS, and the underlying mechanism is closely associated with the inhibition of podocyte injury.

INTRODUCTION

Nephrotic syndrome (NS) is defined by severe proteinuria, hypoalbuminemia, hyperlipemia and edema, which is often associated with acute kidney injury (AKI), thromboembolism and infection [1]. As one of the most common glomerular diseases [2], NS is characterized by the high morbidity, disability rate and death rate despite huge advances in its treatment [3]. For example, as a common pathological type of NS, minimal change disease (MCD) occupies a proportion of 15% in adults, and up to 70–90% in children [4]. Currently, the mechanism of NS is complex and controversial, but podocyte injury is regarded as the central event [5]. As the glomerular epithelial cell, podocyte has been considered as the final gatekeeper of glomerular filtration barrier [6]. Nowadays, glucocorticoids, calcineurin inhibitor, and rituximab are widely used in

clinic, which may in turn cause a series of problems, such as serious adverse effects, economic pressure and frequent recurrence [7]. Therefore, exploring more advanced drugs is crucial in treating NS.

Recently, accumulated evidences further demonstrate traditional Chinese medicine (TCM) is applied in treating NS with therapeutic efficacy, low cost, and few side effects [8–10]. Yuebi Decoction (YBD), a famous traditional Chinese medicine compound, is composed of five Chinese medicinal materials, including *Ephedra sinica Stapf* (Mahuang, MH), *Gypsum Fibrosum* (Shigao, SG), *Zingiber officinale Rosc* (Shengjiang, SJ), *Glycyrrhiza uralensis Fisch* (Gancao, GC) and *Ziziphus jujuba Mill* (Dazao, DZ). Recently, YBD has been reported to show positive effects on decreasing proteinuria, increasing serum albumin, ameliorating renal function, reducing oxidative stress and inflammatory reaction [11, 12]. In clinical research reports, YBD has been proved to treat NS, and the total effective rate was up to 95.00% [13]. Therefore, YBD is widely used in the treatment of NS. MH has antioxidant, anticarcinogen, antibacterial, antidiabetic, anti-obesity, antiarthritic, antiviral and diuretic activities [14, 15]. SG is a promising mineral medicine with antioxidant, antiviral, and immunity-enhancement properties [16]. Similarly, SJ, GC, and DZ have been reported to show pharmacological activities of anti-inflammatory, antioxidant, anti-atherogenic, and antibacterial [17, 18]. However, the mechanism of YBD in treating NS still remains unknown. So, we used bioinformatics and *in vivo* experiment to explore the effect of YBD in treating NS.

As is known, network pharmacology is regarded as an emerging and promising subject to explore the connections between active ingredients and diseases [19]. Through constructing "drug-ingredients-targets-pathways" network, network pharmacology effectively integrates computer technology and systems biology to reveal pharmacological mechanisms of TCM in treating related diseases [20]. In recent years, more and more researches related to TCM are conducted by network pharmacology [21, 22]. Here, active ingredients, targets of YBD in treating NS, and pathways were analyzed. Subsequently, *in vivo* experiment was conducted to verify the results (Figure 1). Our research gives the idea on treating NS and contributes to the clinical application of YBD in the future.

MATERIALS AND METHODS

Exploring of ingredients and potential targets of YBD

Five medicines from YBD, namely, Mahuang, Shigao, Shengjiang, Gancao, and Dazao were respectively inputted into the search box as keywords to retrieve in TCMSP (https://tcmsp-e.com/). Since the average value of oral bioavailability (OB) and drug-likeness (DL) from all molecules in DrugBank is 30% and 0.18 respectively, OB ≥30% and DL ≥0.18 are considered as significant parts in network pharmacology [23]. Then, TCMSP and SwissTargetPrediction were used to predict target proteins of active ingredients (http://www.swisstargetprediction.ch/). Finally, gene names were further mapped via UniProt database.

Establishment of herb-ingredient-target (H-I-T) network

Cytoscape (version 3.9.1) was applied to establish a network between herbs, active ingredients of YBD and targets. As an open software for visualizing, Cytoscape software is widely applied in the field of network pharmacology [24].

Screening of potential targets against NS

The targets were successfully obtained from GeneCards, PharmGKB and OMIM databases. The key word "nephrotic syndrome" was inputted as index words. The repeated targets corresponding to NS and YBD were deleted. Overlapping targets were successfully acquired by Venn diagram.

Establishment of protein-protein interaction (PPI) network

STRING is an online and reliable database, which can be used to predict the interactions between proteins. Overlapping targets were inputted into STRING. In addition, disconnected genes in the network were hidden.

Gene ontology (GO) and kyoto encyclopedia of genes and genome (KEGG) pathway enrichment analyses

GO contains biological process (BP), cellular component (CC), and molecular function (MF) [25, 26]. The Database for Annotation, Visualization and Integrated Discovery (DAVID) and ClueGO were applied to complete this part. The overlapping targets were entered into DAVID.

Molecular docking simulation

To further explore connections between ingredients and targets, molecular docking was conducted. We chose five ingredients with the greatest number of overlapping targets as the ligands. Meanwhile, we selected five core targets as the receptors for verification. We searched for known ligands of protein receptors on the PDB to prepare for molecular docking. Firstly, 2D structures

were acquired. Afterwards, 3D structures (mol2 format) with minimum energy of active ingredients were obtained from Chem3D software and converted into PDB format by PyMOL software as the ligands in molecular docking. Next, the PDB website was used to obtain the 3D structures of core targets. Then, PyMOL software was applied to delete water molecules, and those core targets were saved in PDB format as the receptors in molecular docking. Next, AutoDockTools was applied to convert small molecule ligands and receptors into PDBQT format. Finally, the binding was evaluated through Vina. −5 kcal/mol was set as a threshold affinity in this study.

Experimental validation

Experimental materials and preparation of YBD

The medicinal materials of YBD were provided by Yueyang Hospital. Cyclosporin A (CsA; Lot. H10960008) was purchased from North China
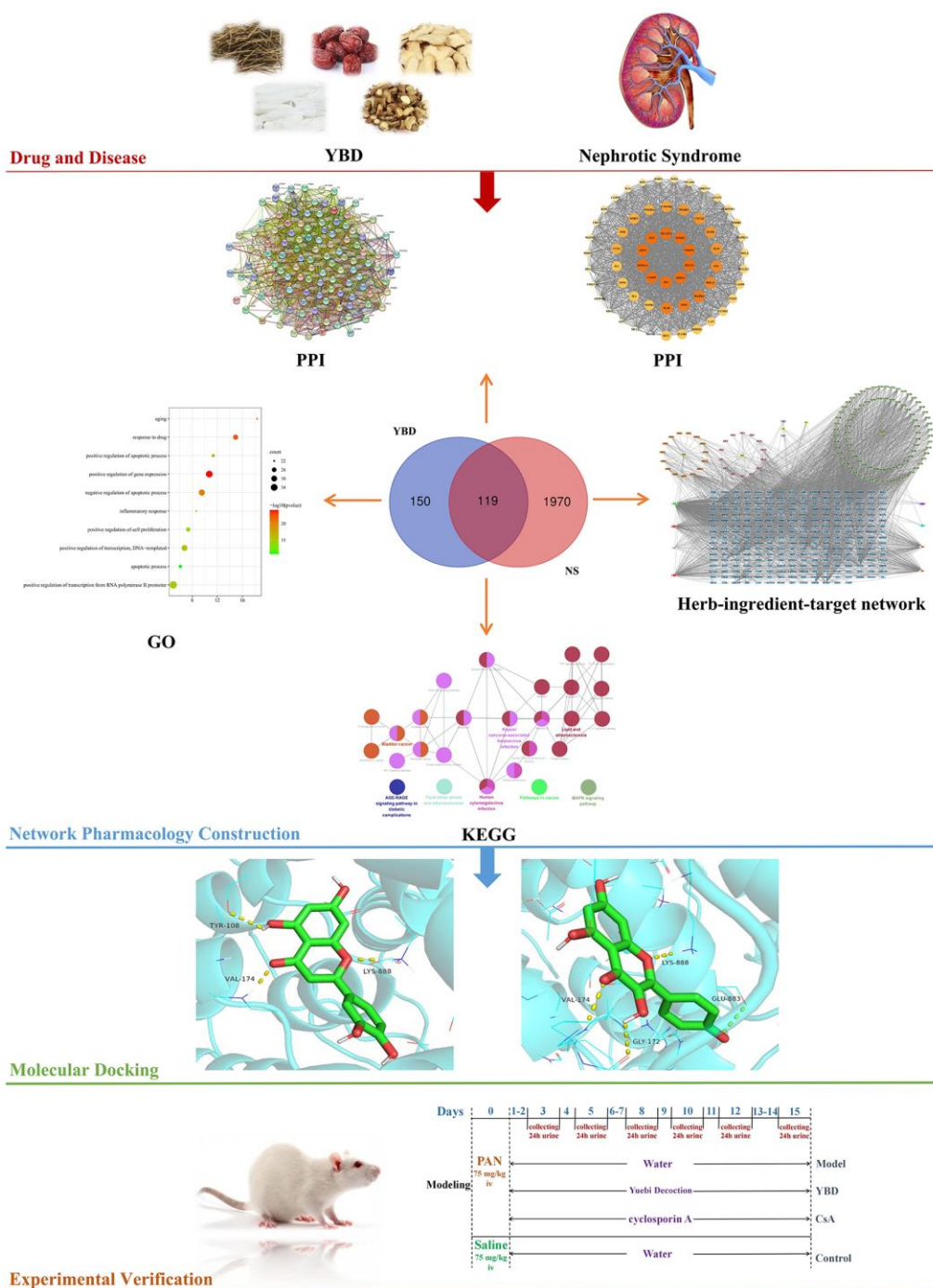

Figure 1. A comprehensive strategy diagram for the study of the mechanism of YBD in treating NS.

Pharmaceutical Co., Ltd (China). Puromycin amino-nucleoside (PAN; Lot. 108M4067V) was purchased from Sigma-Aldrich Co., Ltd. (USA). Podocin (PB9903) and nephrin (BM0676) antibodies were purchased from Boster (China). PPP3CA (YN2056), AKT1 (YN0514), STAT3 (YN0127), NFATC3 (YN0789), and TRPC6 (YN1223) antibodies were purchased from ImmunoWay Biotechnology Company (USA). According to the previous study [27], 660 g YBD were steeped for one hour in 5280 mL distilled water. After that, those dregs were filtered from the first extraction for the second extraction. Three times later, the concentration was 594 mg/mL and kept at 4°C for the further experiment.

Chromatographic analysis of YBD
200 µL YBD (the concentration was 594 mg/mL) was used for ultrasonic dissolution. After centrifugation at temperature of 4°C with 20000 rpm for 10 min, 50 µL was extracted. Then, 450 µL precipitator was added to the supernatant. After centrifugation at temperature of 4°C with 20000 rpm for 10 min, 100 µL sample was applied for LC-MS/MS^2. An UltiMate 3000 RS (Thermo Fisher Scientific) was applied to perform quantitative LC-MS/MS^2 proteomic analysis. Finally, 215 compounds were acquired from YBD via chromatographic analysis (Figure 2), mainly including

quercetin, kaempferol, luteolin, naringenin, formononetin, ephedrine hydrochloride, pseudo-ephedrine hydrochloride, 6-gingerol, isoliquiritigenin, catechin and glycyrrhetinic acid.

Animal model establishment and drug administration

Forty 5 to 6-week-old male Wistar rats weighing 160 ± 20 g were provided by Shanghai SLAC Laboratory Animal Co., Ltd in China (License NO. SCXK 2017–0005). Animal experiment was carried on SPF condition. Those rats were housed under conditions (23 ± 2°C, and 12 h/12 h light/dark cycle) with free access to standard rat chow and water [28]. The urine protein tests of the rats were negative. As shown in Figure 3, except 10 rats in the Control group, other rats were injected with PAN to establish NS model [29]. PAN has non-immune renal damaging effects and can induce the development of podocyte injury. It can cause the extensive fusion of foot processes, and lead to local cells stripped and exposed from the glomerular basement membrane (GBM). Rats in other groups received a single intravenous injection of PAN (75 mg/kg, dissolved in saline). Afterwards, those successful model were divided into three groups (each group includes 10 rats). The 24 h proteinuria was detected to ensure that there was no intergroup difference before treatment.
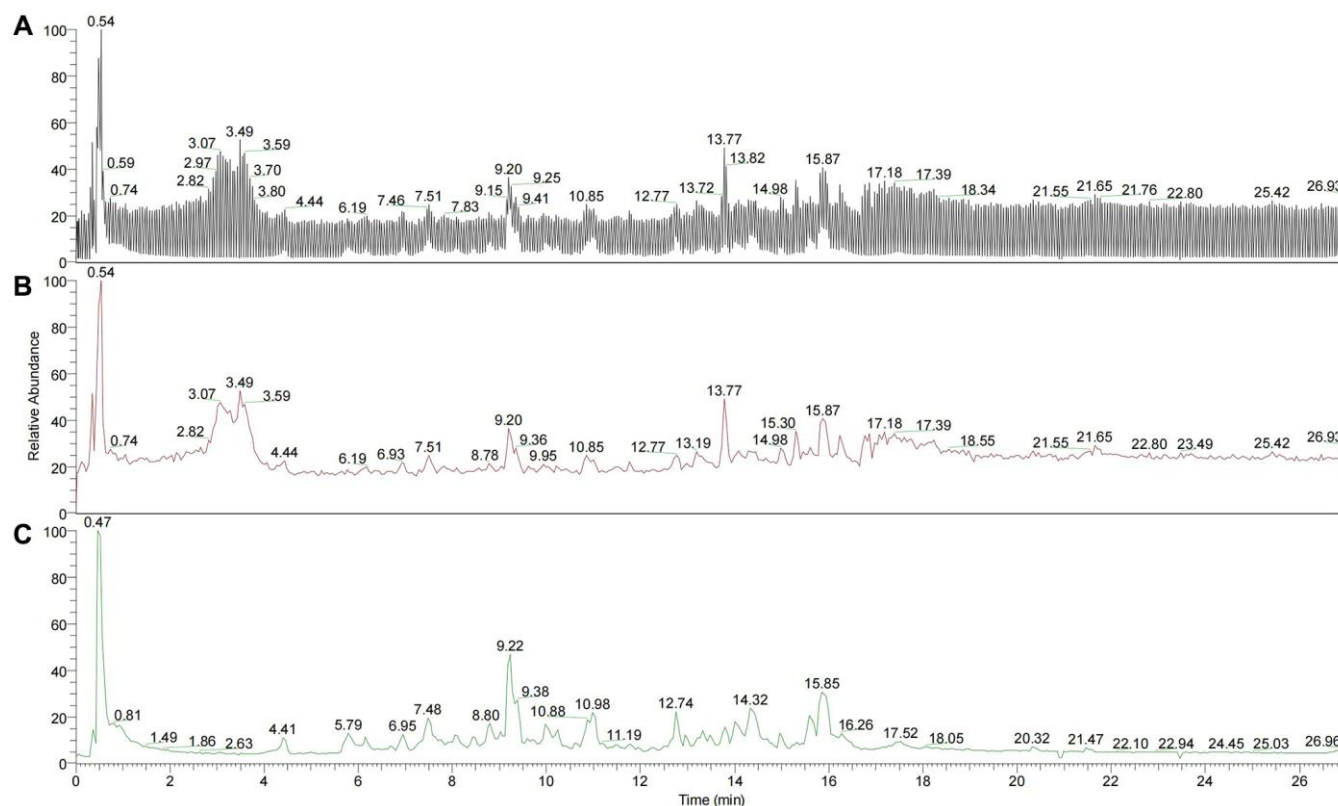

Figure 2. Total ion flow diagram of YBD. (**A**) Total negative and positive ion flow diagram superposition of YBD. (**B**) Total negative ion flow diagram of YBD. (**C**) Total positive ion flow diagram of YBD.

Table 1. Constituents of YBD.

Number	Medicinal materials	Pharmaceutical name	Part used	Proportion
1	Ma Huang	Ephedra sinica Stapf	stem	6
2	Shi Gao	Gypsum Fibrosum	mineral	8
3	Sheng Jiang	Zingiber officinale Rosc	rhizome	3
4	Gan Cao	Glycyrrhiza uralensis Fisch	radix	2
5	Da Zao	Ziziphus jujuba Mill	fruit	3

Since calcineurin inhibitors (CNIs) served as a common strategy in treating NS, we chose CsA as the positive drug. For example, YBD was composed of five Chinese medicinal materials in Table 1, and it was taken 66 g daily for a patient with 70 kg weight in clinical. According to the equivalent dose of human and rats, the dose of rats = 66000 mg/kg/d × 0.018/0.2 kg, the same method was used to calculate the dose of CsA [30]. Drug treatments of each group were performed once daily for 15 days.

Measurement of urinary protein, blood pressure, and serum biochemical analysis

At the end of the 3th, 5th, 8th, 10th, 12th and 15th day, the 24 h urine specimens were collected. Before the treatment and after 15 days of medicine treatment, the arterial pressure on the tails of rats was measured by noninvasive blood pressure collection system (BP-98A). Each rat was measured 3 times and the average level of blood pressure was calculated. When measuring the blood pressure, we waited 3 minutes for the rats to calm down. All the rats were sacrificed after the last treatment. Blood samples were obtained after the rats were anesthetized with pentobarbital sodium [31].

F-actin cytoskeleton staining

Antigen retrieval was completed by Ethylene Diamine Tetraacetic Acid (EDTA) for kidney sections from different groups. Then, those sections were incubated with primary anti-F-actin. Afterwards, they were washed 3 times by PBS. Fifty minutes later, Actin-Tracker Green and DAPI were used to stain cell cytoskeleton and nucleus, respectively [32]. Under the microscope, F-actin was shown green by the tracer and the nucleus was stained blue by DAPI. Finally, Image Pro PLus 6.0 was used to analysis images. Colorful fluorescent images were first converted to black and white. Then, the same black color was chosen as a uniform standard for determining positivity, and the glomerular areas in images were segmented. Subsequently, the cumulative integrated optical density (IOD) and corresponding areas of the positive parts in images were acquired. IOD/AREA was calculated in each group.

Western blotting analysis

Protein concentration was detected by BCA Protein Assay Kit. Then, total proteins were separated through
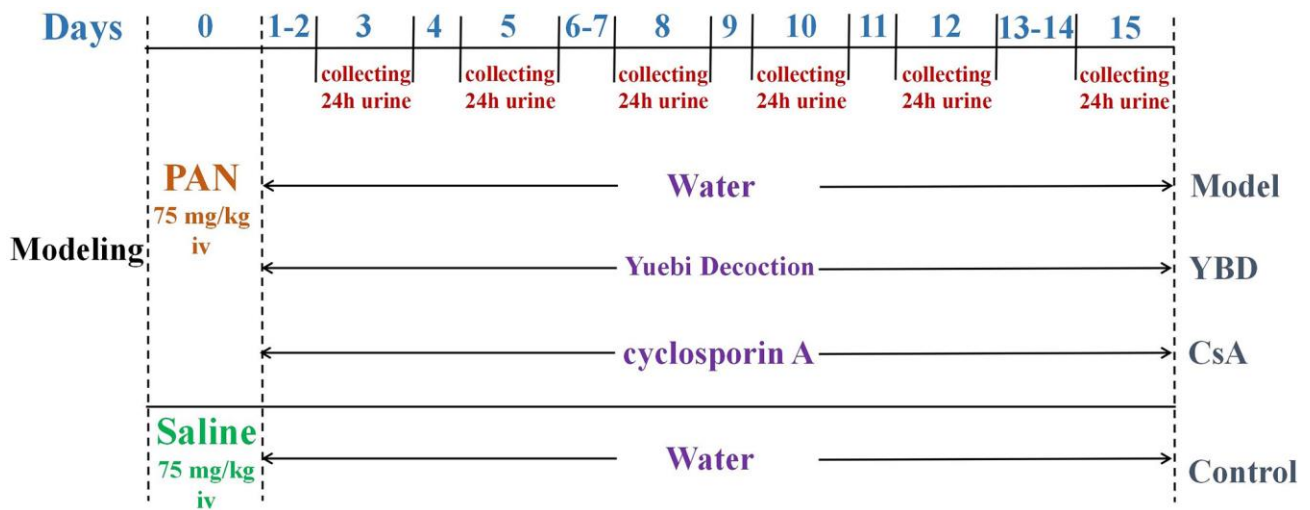

Figure 3. The schematic representation of brief experimental schedule including modeling and treatment. After acclimatization, 10 rats were randomly assigned to the Control group and intravenously injected with saline (75 mg/kg). Meanwhile, other rats were intravenously injected with PAN (75 mg/kg) to establish NS model on day 0. In the subsequent fifteen days, they were orally administered distilled water, YBD or CsA respectively.

10% SDS-PAGE. The membranes were incubated with the antibodies of podocin (1:1000), nephrin (1:1000), PPP3CA (1:1000), STAT3 (1:1000), NFATC3 (1:1000), TRPC6 (1:1000), and AKT1 (1:1000). Finally, the membranes were washed by a multi-functional imaging system (Tanon-5200).

Statistical analysis

SPSS 21.0 software was used for statistical analysis. Data were presented as mean ± SD. Comparisons among groups were made via ANOVA followed by Duncan's test. Values with $p < 0.05$ were considered statistically significant.

Data availability statement

The data used to support the findings of this study are available from the corresponding author upon request.

RESULTS

Ingredients of YBD and their potential targets

124 different ingredients from YBD were obtained from TCMSP and literature research in this study. There were 22 active ingredients from MH, 19 active ingredients from DZ, 5 active ingredients from SJ, 1 active ingredient from SG, and 88 active ingredients from GC. Detailed information was provided in Supplementary Table 1. 269 targets of the active ingredients were acquired through SwissTargetPrediction and TCMSP. Detailed information was provided in Supplementary Table 2. Obviously, quercetin, kaempferol, luteolin, naringenin, beta-sitosterol, 7-Methoxy-2-methyl isoflavone, stigmasterol, isorhamnetin, formononetin, and licochalcone A were top ten ingredients, which had the greatest number of targets. Then, their CAS number, and chemical structure were provided in Table 2. Finally, in the network, there were 397 nodes (5 herbs, 124 active ingredients, and 269 targets) and 2570 edges (Figure 4).

Screening of overlapping targets

2089 NS-related targets were acquired through the public databases. Besides, 119 overlapping genes of between YBD and NS were acquired by a Venn diagram, which were regarded as potential therapeutic targets of YBD against NS (Figure 5). Detailed information was provided in Supplementary Table 3.

PPI network and core targets

In Figure 6A, the PPI network included 118 nodes and 2595 edges. In Figure 6B, 59 core targets were acquired with value greater than 44.0. After putting 59 core targets into Cytoscape, we found a majority of them were related to podocyte injury, and the top ten targets were AKT1, STAT3, TRPC6, CASP3, JUN, PPP3CA, IL6, PTGS2, VEGFA, and NFATC3.
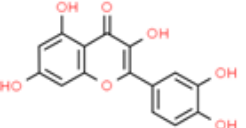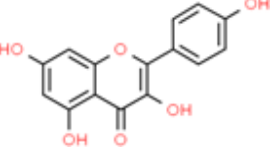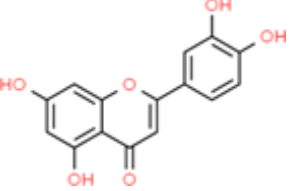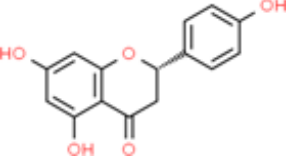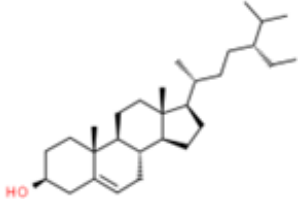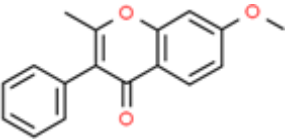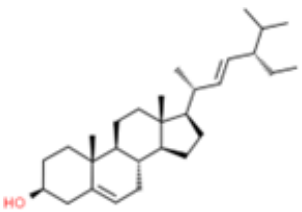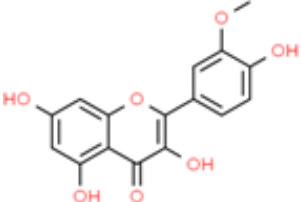
GO and KEGG analysis

GO indicated that those targets were enriched in 513 BP, 89 CC, and 114 MF. In the BP ontology, the targets primarily associated with positive regulation of apoptotic process, apoptotic process, inflammatory response, aging (Figure 7A). In the CC ontology, the targets located mainly in cytosol, cytoplasm, nucleus, mitochondrion, and membrane (Figure 7B). In the MF ontology, it could be seen that the targets were mainly involved in protein homodimerization activity, protein kinase binding, macromolecular complex binding, and transcription factor activity (Figure 7C). Detailed information on GO enrichment analysis was performed in Supplementary Table 4.
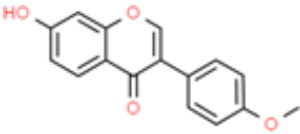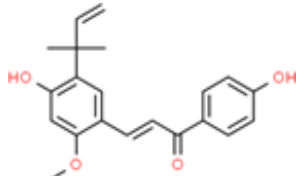
Finally, we acquired 27 representative pathways as shown in Figure 8. Those significant pathways could be divided into 8 categories, including AGE-RAGE signaling pathway in diabetic complications, MAPK signaling pathway, Fluid shear stress and atherosclerosis, Human cytomegalovirus infection, and Pathways in cancer.

Molecular docking

Quercetin, kaempferol, luteolin, naringenin, and beta-sitosterol were regarded as ligands. Then, we selected AKT1, TRPC6, STAT3, PPP3CA, and NFATC3 as the protein receptors because they belonged to the top ten targets. Meanwhile, they were involved in development of podocyte injury and became critical targets in the treatment of NS through participating in many key biological processes including molecular trafficking, receptor activation, and signal transduction. The detailed information on the known ligands of AKT1, TRPC6, STAT3, PPP3CA, and NFATC3 were performed in Supplementary Table 5. In Table 3, quercetin owned the best affinity of −8.0 with TRPC6 and −7.8 with NFATC3. Kaempferol owned the best affinity of −8.1 with TRPC6 and −7.7 with PPP3CA. Luteolin owned the best affinity of −8.2 with TRPC6, −7.6 with STAT3, and −7.6 with PPP3CA. Naringenin owned the best affinity of −7.5 with TRPC6 and −7.4 with PPP3CA. Beta-sitosterol owned the best affinity of −7.0 with PPP3CA and −6.8 with TRPC6. Compared with affinity of the known ligand and its corresponding target, it showed that YBD had strong effects on its targets (Figure 9).

Table 2. Information table of top ten active ingredients of YBD.

CAS number	Ingredient name	Chemical structure	Molecular formula	Molecular weight
117-39-5	Quercetin		$C_{15}H_{10}O_7$	302.24
520-18-3	Kaempferol		$C_{15}H_{10}O_6$	286.24
491-70-3	Luteolin		$C_{15}H_{10}O_6$	286.24
480-41-1	Naringenin		$C_{15}H_{12}O_5$	272.25
83-46-5	Beta-sitosterol		$C_{29}H_{50}O$	414.71
19725-44-1	7-Methoxy-2-methyl isoflavone		$C_{17}H_{14}O_3$	266.31
83-48-7	Stigmasterol		$C_{29}H_{48}O$	412.69
480-19-3	Isorhamnetin		$C_{16}H_{12}O_7$	316.28

485-72-3	Formononetin		$C_{16}H_{12}O_4$	268.28
58749-22-7	Licochalcone A		$C_{21}H_{22}O_4$	338.43

Verification of the effect of YBD on NS *in vivo*

Effects of YBD on proteinuria, urine volume, and blood pressure in NS rats

We detected 24 h urine protein and urine volume at various time points, and found that proteinuria levels in the Model group peaked on day 10. However, YBD group exhibited a significant decline in 24 h proteinuria compared with the Model group from day 5 to day 15 ($p < 0.01$). While, CsA produced similar results compared with YBD (Figure 10A). Besides, we also found that YBD had an effect on urine volume. YBD significantly increased 24 h urine volume compared with the Control group from day 5 to day 15 ($p < 0.05$) (Figure 10B). To observe the effect of YBD on blood pressure, we compared the changes of SBP and DBP between each group. Before the treatment, no difference was exhibited on the level of SBP and DBP between the four groups (Figure 10C, 10E). After the treatment, it was found that DBP of rats treated with YBD decreased compared with the Model group ($p < 0.05$) (Figure 10F). Besides, SBP of rats in the YBD group decreased compared with the Model group. However, no difference was found on the level of SBP between the two groups (Figure 10D).
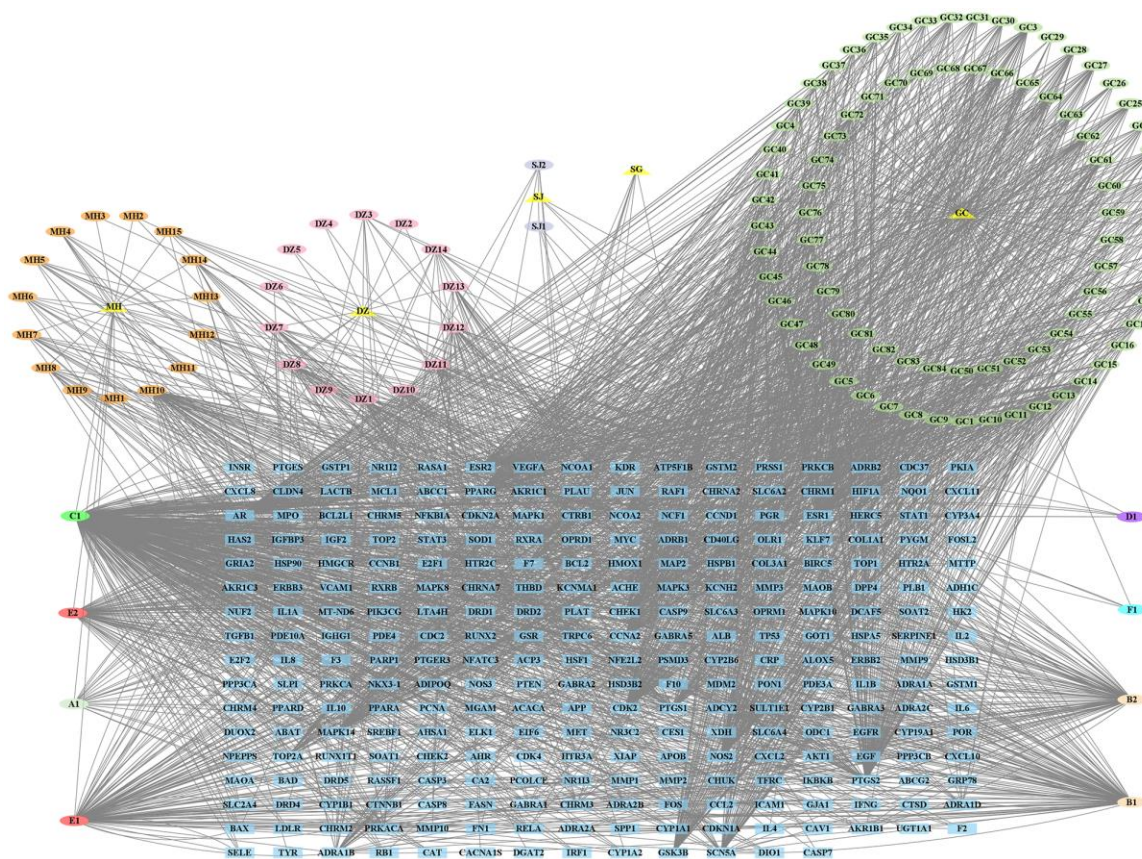
Figure 4. Herb-ingredient-target network of YBD. The yellow triangle nodes represented herbs, the green, orange, pink, gray, purple oval nodes represented different ingredients, and the blue rectangle nodes represented targets.
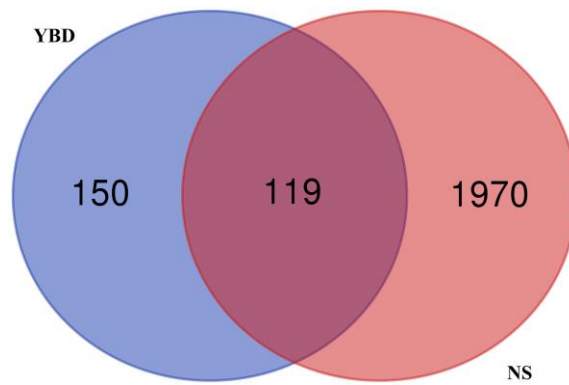
Figure 5. Venn diagram of overlapping targets on YBD and NS. The blue circle represented the targets of YBD, and the red circle represented the targets of NS. The part of the two intersecting circles represented the overlapping targets.
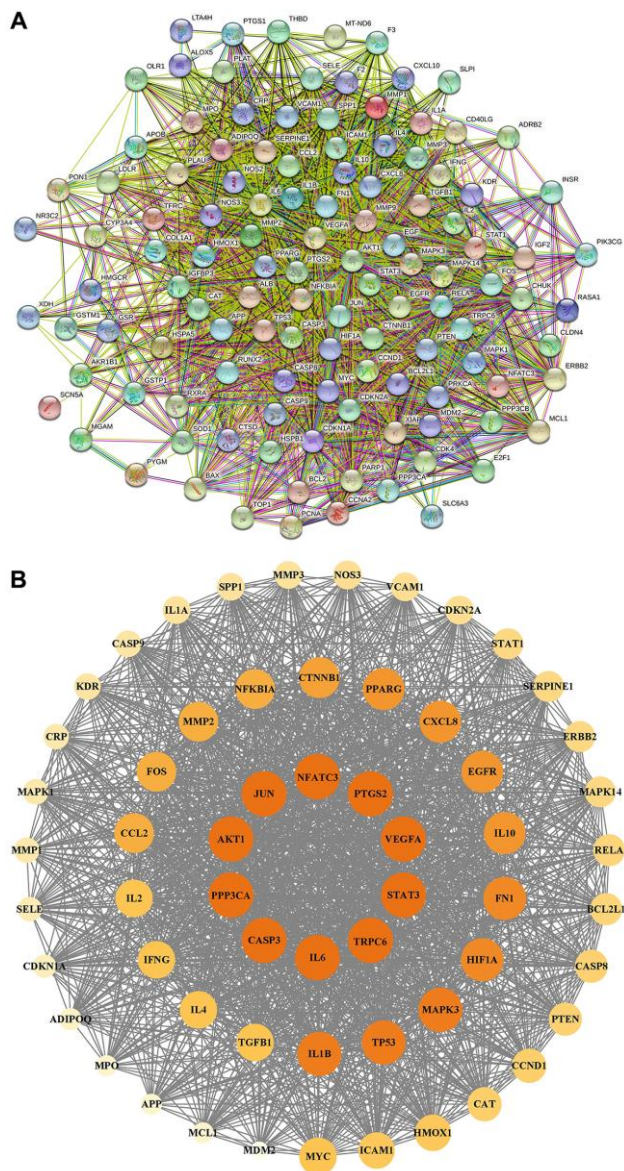
Figure 6. PPI network construction. (**A**) PPI network of potential therapeutic targets for YBD against NS through STRING database. (**B**) PPI network of core targets for YBD against NS through Cytoscape software. Colors from faint yellow to deep yellow are proportional to the degrees of nodes.
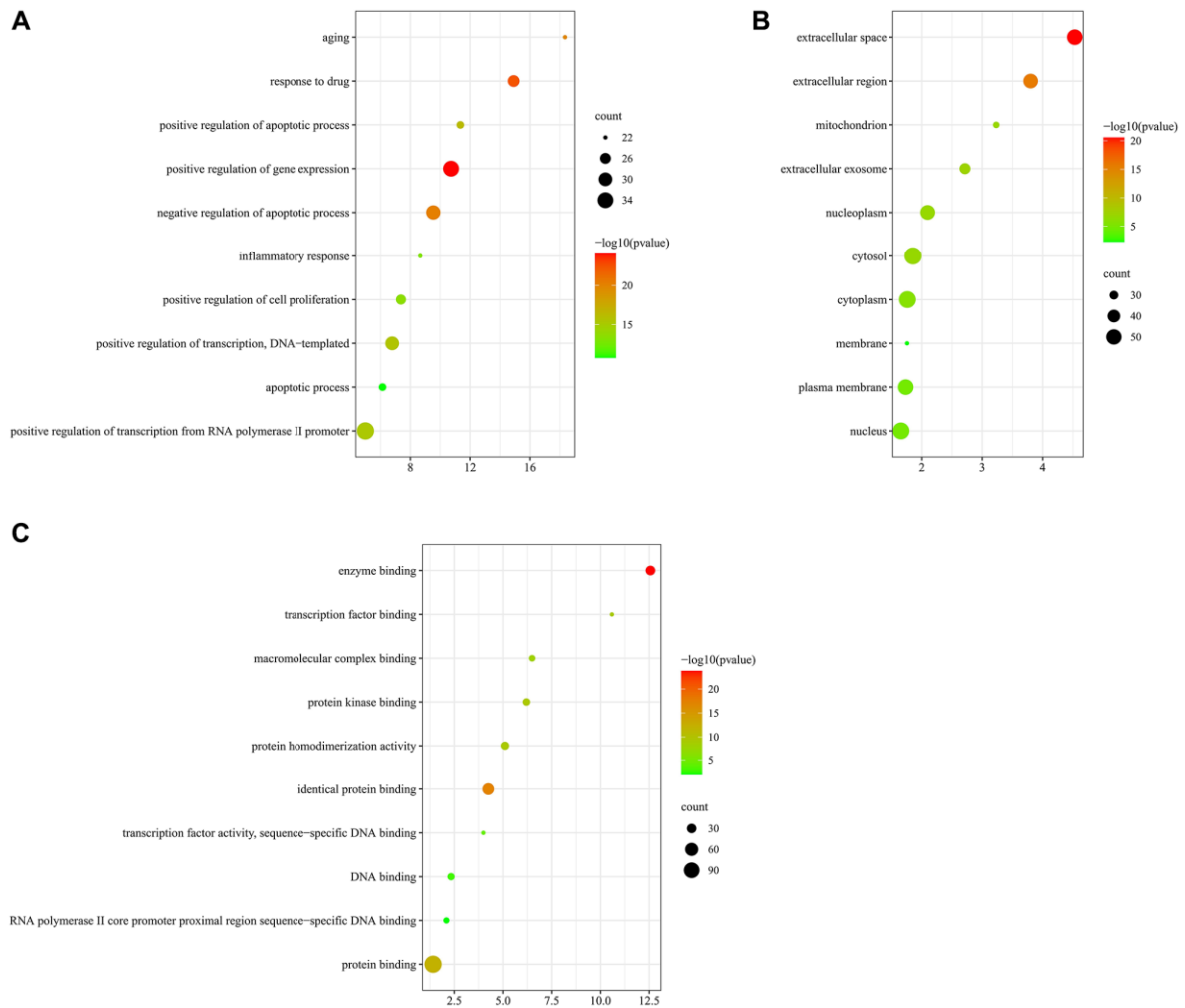
Figure 7. GO enrichment analysis of 119 overlapping targets by DAVID database. (**A**) the top 10 enriched terms in BP. (**B**) The top 10 enriched terms in CC. (**C**) The top 10 enriched terms in MF.
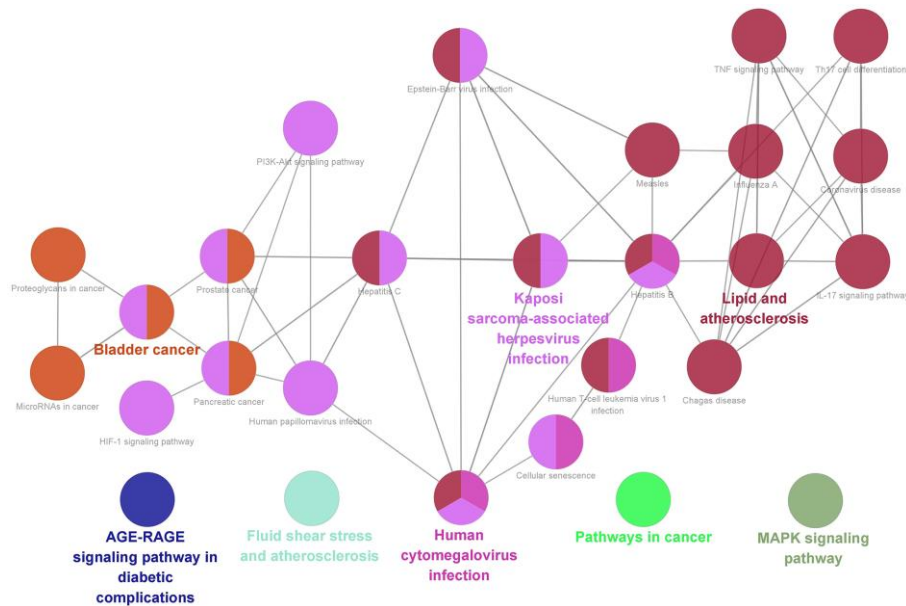
Figure 8. KEGG pathway analysis of 119 overlapping targets through ClueGO.

Table 3. Molecular docking scores of main active ingredients and targets.

Group	AKT1	TRPC6	STAT3	PPP3CA	NFATC3
Quercetin	−5.7	−8.0	−7.4	−7.7	−7.8
Kaempferol	−6.1	−8.1	−7.4	−7.7	−7.0
Luteolin	−6.2	−8.2	−7.6	−7.6	−7.3
Naringenin	−6.2	−7.5	−7.0	−7.4	−6.8
Beta-sitosterol	−5.0	−6.8	−6.4	−7.0	−5.0
Positive control	−6.2	−8.0	−7.1	−7.8	−8.2

Effects of YBD on ALB, BUN, SCr, SUA and serum lipid

As a remarkable symptom in NS, hypoalbuminemia was extremely showed in PAN-induced rats. Model group exhibited an decreased level of ALB when compared with Control group ($p < 0.01$). Both YBD and CsA groups had significantly increased the level of ALB compared with Model group ($p < 0.01$) (Figure 11A). YBD could improve renal function to some extent (Figure 11B–11D). The levels of BUN and SCr increased in Model group compared with Control group ($p < 0.01$). The levels of SCr and BUN decreased in YBD administration group compared with Model group ($p < 0.01$). TC, TG and LDL-C increased in Model group compared with Control group ($p < 0.01$). YBD could significantly decrease TC, TG and LDL-C compared with Model group ($p < 0.01$) (Figure 11E–11G)). While, no difference was exhibited on HDL-C between four groups (Figure 11H).

Effects of YBD on histopathological changes in NS rats

Through light microscopy, there were no significant histopathologic abnormalities in the glomerular structures among all groups. Model group exhibited abundant protein exudation in renal tubular lumens and inflammatory cell infiltration. However, YBD could attenuate the pathological damage through reducing protein cast formation and inflammatory cell (Figure 12A, 12B)). The transmission electron microscopy showed more clear morphological ultrastructure changes of podocyte (Figure 12C). Normal podocyte architecture could be seen in the Control group. However, injection of PAN evidently caused the massive effacement and extensive fusion of podocyte foot processes in the Model group. When treated with YBD, the effacement and fusion of foot processes significantly decreased.

Effects of YBD on marker proteins of podocyte injury in NS rats

We observed that PAN destroyed the amount and structure of F-actin stress fibers compared with Control group ($p < 0.01$). YBD could restore the amount of F-actin stress fibers and their structure prominently compared with Model group ($p < 0.01$) (Figure 13A, 13B). The decreased expression of nephrin or podocin is a hallmark of podocyte injury [33–35]. Western blotting was performed in this study to detect the expressions of nephrin and podocin. The expressions of podocin and nephrin markedly decreased in Model group compared with Control group. However, YBD could restore the low expressions of podocin and nephrin compared with Model group ($p < 0.05$) (Figure 13C, 13D).

Effects of YBD on the expression levels of core targets

Five core targets (PPP3CA, STAT3, NFATC3, TRPC6, and AKT1) were collected as therapeutic targets of YBD. We examined the protein expressions of PPP3CA, STAT3, NFATC3, TRPC6, and AKT1 in renal tissues (Figure 14). Rats in Model group exhibited higher expressions of PPP3CA, STAT3, NFATC3, TRPC6, and AKT1 when compared with Control group ($p < 0.01$). However, after the treatment of YBD, PPP3CA, NFATC3, and TRPC6 in YBD group greatly decreased compared with Model group ($p < 0.01$). YBD could decrease high expressions of STAT3 and AKT1 compared with Model group ($p < 0.05$). Obviously, these indicated that YBD had protective effects on NS by improving podocyte injury.

DISCUSSION

Proteinuria is an important marker of renal progression and acts as a key point in the clinical treatment. Recently, podocyte injury has gained acceptance as a key target leading to NS [36–38]. The highly differentiated polarized cell has a main body which bulges into the urinary space. In addition, podocyte injury is also regarded as an independent risk factor for the progression of renal diseases [39]. So, improving injured podocyte is crucial to the successful treatment of NS. Although corticosteroid and other immuno-suppressive drugs have significantly reduced the risk of NS, it still remains unacceptably high morbidity in affected patient populations [40]. So, over the last
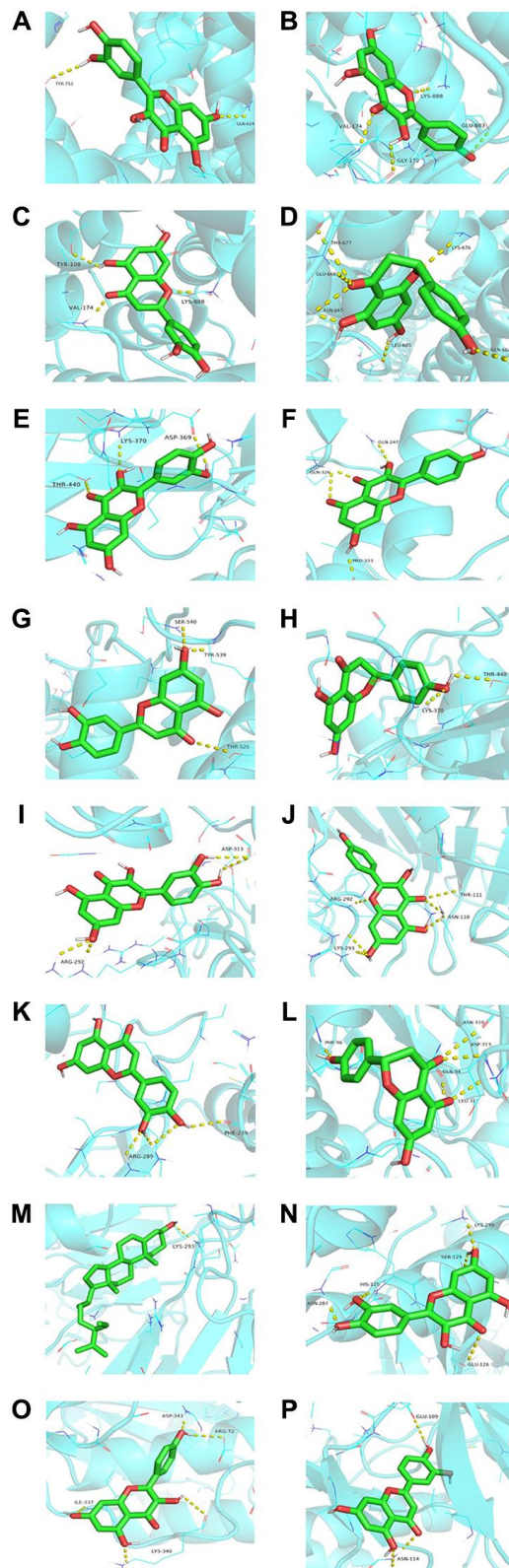
Figure 9. Molecular docking of representative ingredients and targets (the affinity energy is less than or equal to −7.0 kcal/mol). (**A**) Quercetin acts on TRPC6. (**B**) Kaempferol acts on TRPC6. (**C**) Luteolin acts on TRPC6. (**D**) Naringenin acts on TRPC6. (**E**) Quercetin acts on STAT3. (**F**) Kaempferol acts on STAT3. (**G**) Luteolin acts on STAT3. (**H**) Naringenin acts on STAT3. (**I**) Quercetin acts on PPP3CA. (**J**) Kaempferol acts on PPP3CA. (**K**) Luteolin acts on PPP3CA. (**L**) Naringenin acts on PPP3CA. (**M**) Beta-sitosterol acts on PPP3CA. (**N**) Quercetin acts on NFATC3. (**O**) Kaempferol acts on NFATC3. (**P**) Luteolin acts on NFATC3. The molecule was represented in a ball-stick model with atoms C and O in green and red, respectively.

two decades, numerous studies have been performed to study mechanisms of TCM in treating NS. YBD is a famous compound formula recorded in "Treatise on Febrile and Miscellaneous Diseases", which has been applied in treating various forms of diseases related to edema and dysuria for years. Recently, we tried to use YBD in the treatment of NS and got a satisfied therapeutic effect. However, the multicomponent and multitarget characteristics, and underlying mechanism of YBD remains unknown.

Network pharmacology is a thriving interdisciplinary science and technology [41]. Through network pharmacology, 124 active ingredients and 119 overlapping
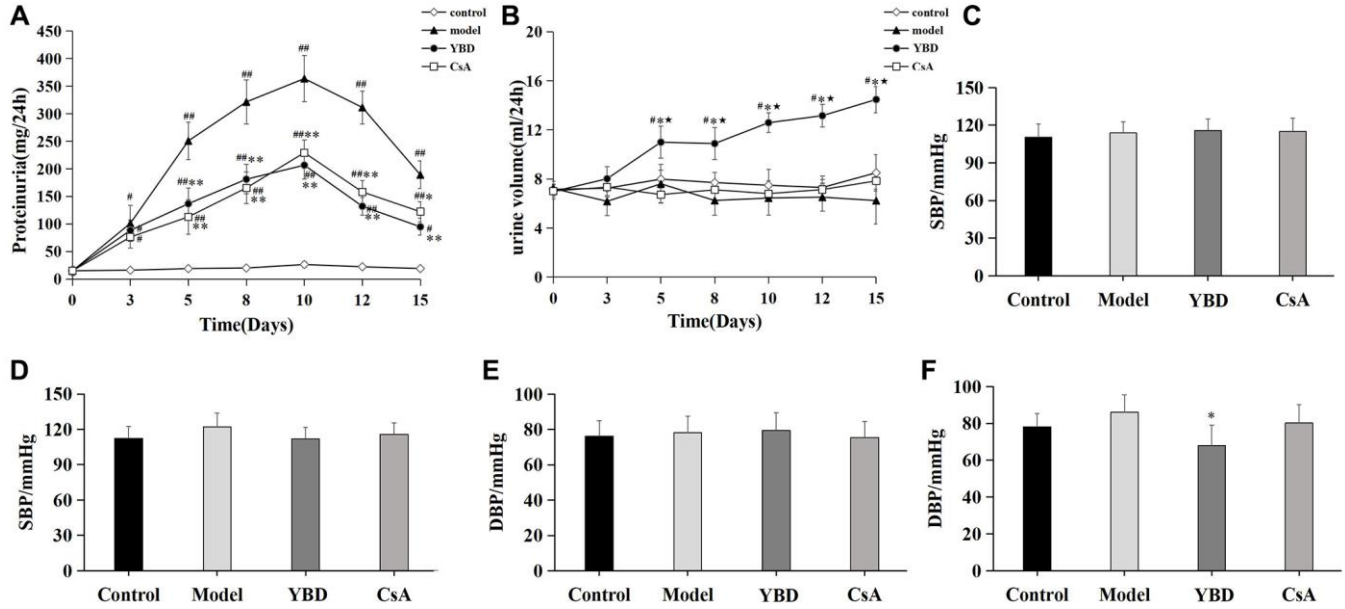
Figure 10. Effects of YBD on proteinuria, urine volume, and blood pressure in NS rats induced by PAN. (**A**) Effects of YBD on 24 h urinary protein excretion at various time points. (**B**) Effects of YBD on 24 h urine volume at various time points. (**C**) Systolic blood pressure (SBP) of rats before the treatment. (**D**) SBP of rats after the treatment. (**E**) Diastolic blood pressure (DBP) of rats before the treatment. (**F**) DBP of rats after the treatment. Data were expressed as mean ± SD, n = 10. Vertical bars represent the standard deviation. $^{#}p < 0.05$ and $^{##}p < 0.01$ versus control group; $^{*}p < 0.05$ and $^{**}p < 0.01$ versus model group; $^{★}p < 0.05$ versus CsA group.
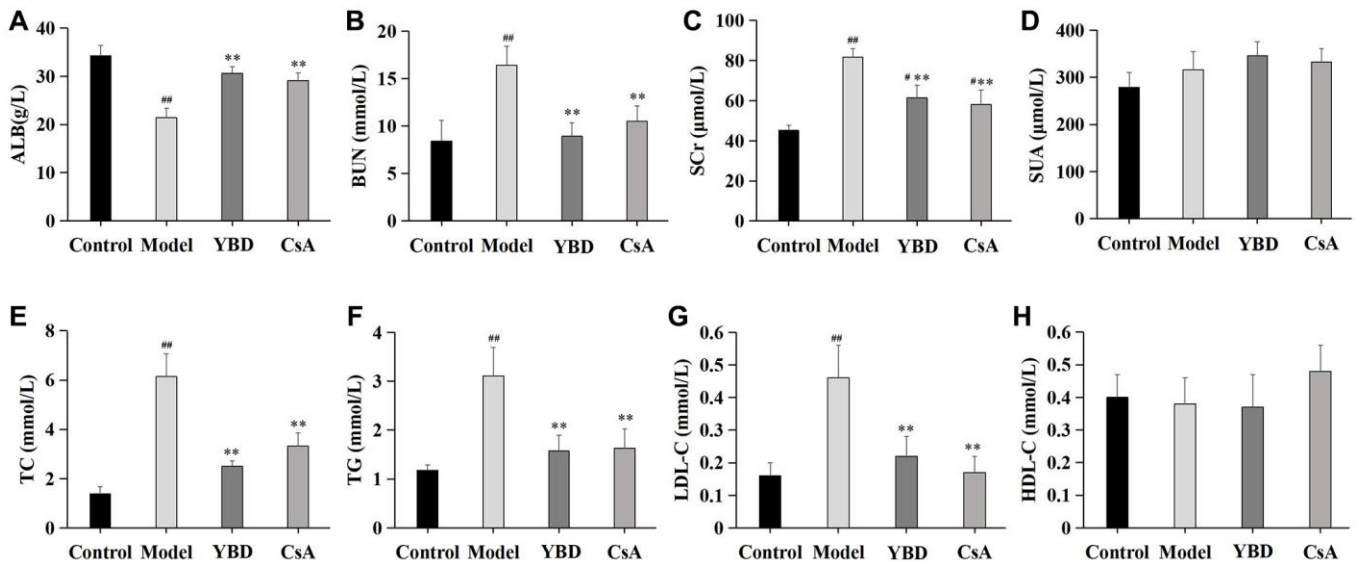
Figure 11. Effects of YBD on albumin (ALB), renal function, and serum lipid in NS rats induced by PAN. (**A**) The indexes of ALB in the serum. (**B–D**) The serum levels of renal function indicators (BUN, SCr, and SUA). (**E–H**) The serum lipid levels (TC, TG, LDL-C, and HDL-C) of each group. Data were expressed as mean ± SD, n = 10. Vertical bars represent the standard deviation. $^{#}p < 0.05$ and $^{##}p < 0.01$ versus control group; $^{*}p < 0.05$ and $^{**}p < 0.01$ versus model group.

targets were identified. The top ten were screened out, such as quercetin, kaempferol, luteolin, naringenin, beta-sitosterol, etc., As one of most important bio-flavonoids, quercetin has positive effects on the biological processes and human health [42]. Quercetin can be extracted from MH, DZ, and GC, which could attenuate the level of podocyte apoptosis, and reduce the expression of pro-apoptotic protein Bax [43]. Kaempferol, a highly purified flavonoid active monomer, can been extracted from many edible plants and TCM, including MH and GC [44]. It has been demonstrated that kaempferol can reduce podocyte apoptosis and improve proteinuria, which is achieved by their modulation on M1/M2 polarization and the lowering effects on levels of IL-1β and TNF-α [45]. Luteolin is also the important ingredient of MH. It has a wide range of biological effects, including anti-oxidative, and anti-inflammatory properties [46]. Luteolin has been reported in combination with prednisone for the treatment of NS [47], and its

underlying mechanism is connected with the inhibition of podocyte injury by regulating NLRP3 inflammasome [48].

AKT1, STAT3, TRPC6, CASP3, JUN, PPP3CA, IL6, PTGS2, VEGFA, and NFATC3 were the top 10 targets. Previous researches have confirmed that some of these targets were closely related to the pathogenic process of NS via participating in podocyte injury [49]. For example, as one of the most important components of TRPC family, TRPC6 has been regarded as the key target for the development of therapeutic agents to NS [50]. On mechanism, TRPC6 is known as a multiple transmembrane protein that mediates the release of cytosolic calcium [51]. The abnormal expression of TRPC6 is most commonly associated with podocyte injury and will accelerate the progression of NS. [52]. When TRPC6 is up-regulated, it would cause the excessive release of cytosolic calcium from podocyte [53]. With the entry of calcium, the expression of
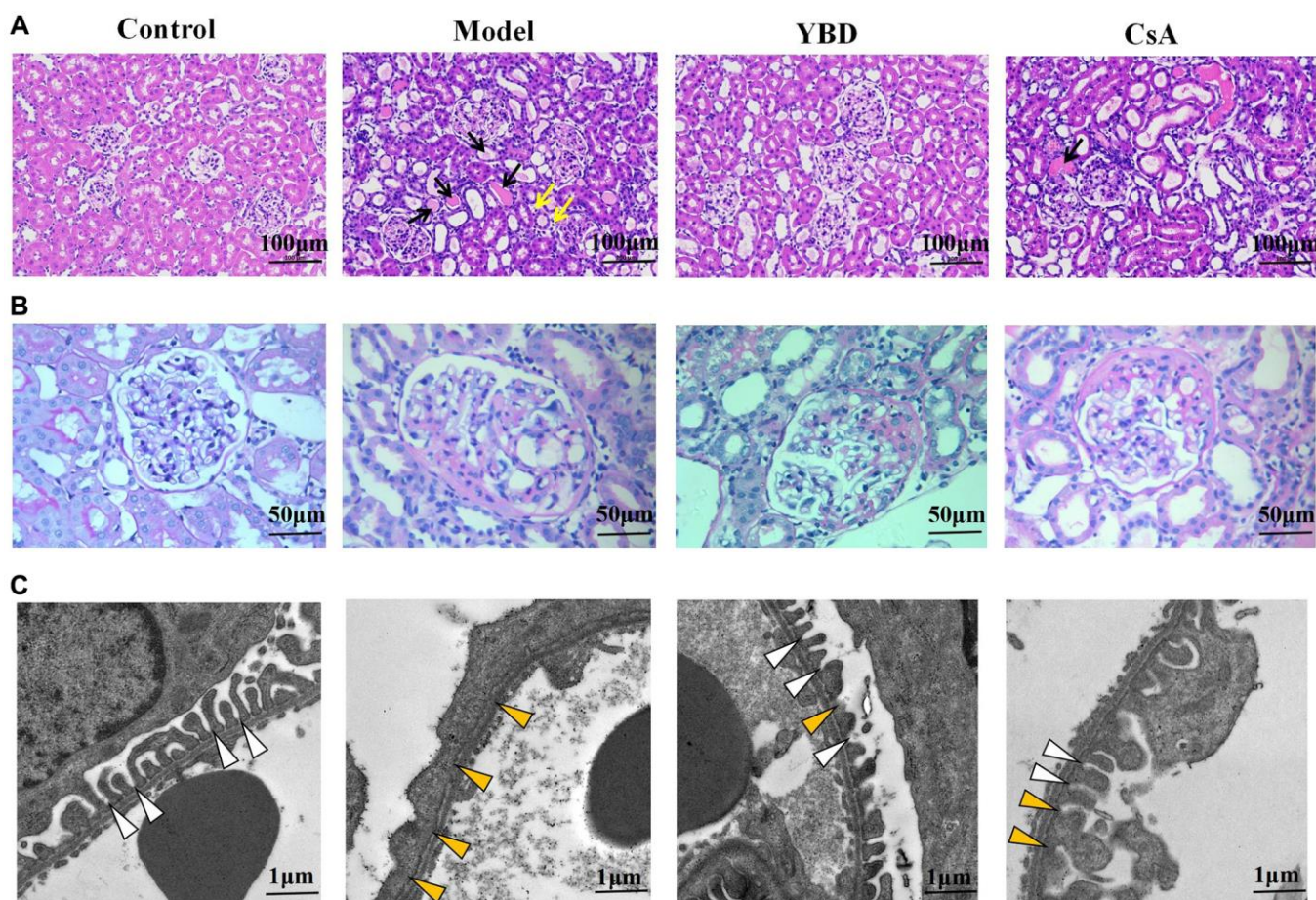
Figure 12. Effects of YBD on renal histopathology in NS rats. (**A**) Morphological observations with HE-stained in renal tissue of the four different groups (magnification×200). Protein casts were indicated by black arrows and inflammatory cell infiltration was indicated by yellow arrows. (**B**) Morphological observations with PAS-stained in renal tissue of the four different groups (magnification × 400). (**C**) Representative images of podocyte foot processes observed by transmission electron microscopy in different groups. The magnification of transmission electron microscopy was 5000. The normal structure of foot processes was marked by white arrow head, the effacement and fusion of foot processes were marked by yellow arrow head.

PPP3CA is promoted under the intervention of TRPC6 [54]. Afterwards, consequent translocation of NFATC3 to the nucleus happens, which further leads to the low expression levels of nephrin, podocin and F-actin [55]. Finally accompanied by fusion of podocyte foot processes, cytoskeleton injury and apoptosis of podocyte were found [56]. Abnormal activation of STATA3 results in podocyte injury and proteinuria [57, 58]. AKT1 is essential to maintain podocyte viability and function during the progression of NS, and through stimulating AKT1 phosphorylation, podocyte apoptosis can be inhibited [59].

Furthermore, GO showed that core targets functioned in the regulation of cell apoptotic process, including podocyte. It is precisely because of podocyte injury that leads to the damage of glomerular filtration barrier and gradually underlies the pathophysiology of NS [60, 61]. Therefore, it is believed that the efficacy of YBD in treating NS is associated with inhibition of podocyte injury. In KEGG pathway enrichment analysis, targets were enriched in AGE-RAGE signaling pathway, MAPK signaling pathway, and pathways in cancer. For example, AGE-RAGE plays a major role in pathophysiology of NS caused by diabetes. It has been reported that abnormal activation of AGE-RAGE stimulates NADPH oxidase-mediated reactive oxygen species production, leading to glomerular hypertrophy, podocyte injury, and mass proteinuria [62]. MAPK is closely associated with the disruption of cytoskeletal proteins (podocin and nephrin), endoplasmic reticulum stress activation, and apoptosis, which is an important pathway in treating NS [63].

Molecular docking is a significant method to predict the affinity [64]. It could be found that the energy of main ingredients to core proteins was no more than −5.0 kcal/mol. According to Figure 8, quercetin, kaempferol, and luteolin could closely bind to the various targets, such as AKT1, TRPC6, STAT3, PPP3CA, and NFATC3. Obviously, the best binding affinity (−8.2 kcal/mol) was observed between luteolin and TRPC6, which mainly depended on the hydrogen bond interaction with TYR-108, VAL-174, and LYS-888.
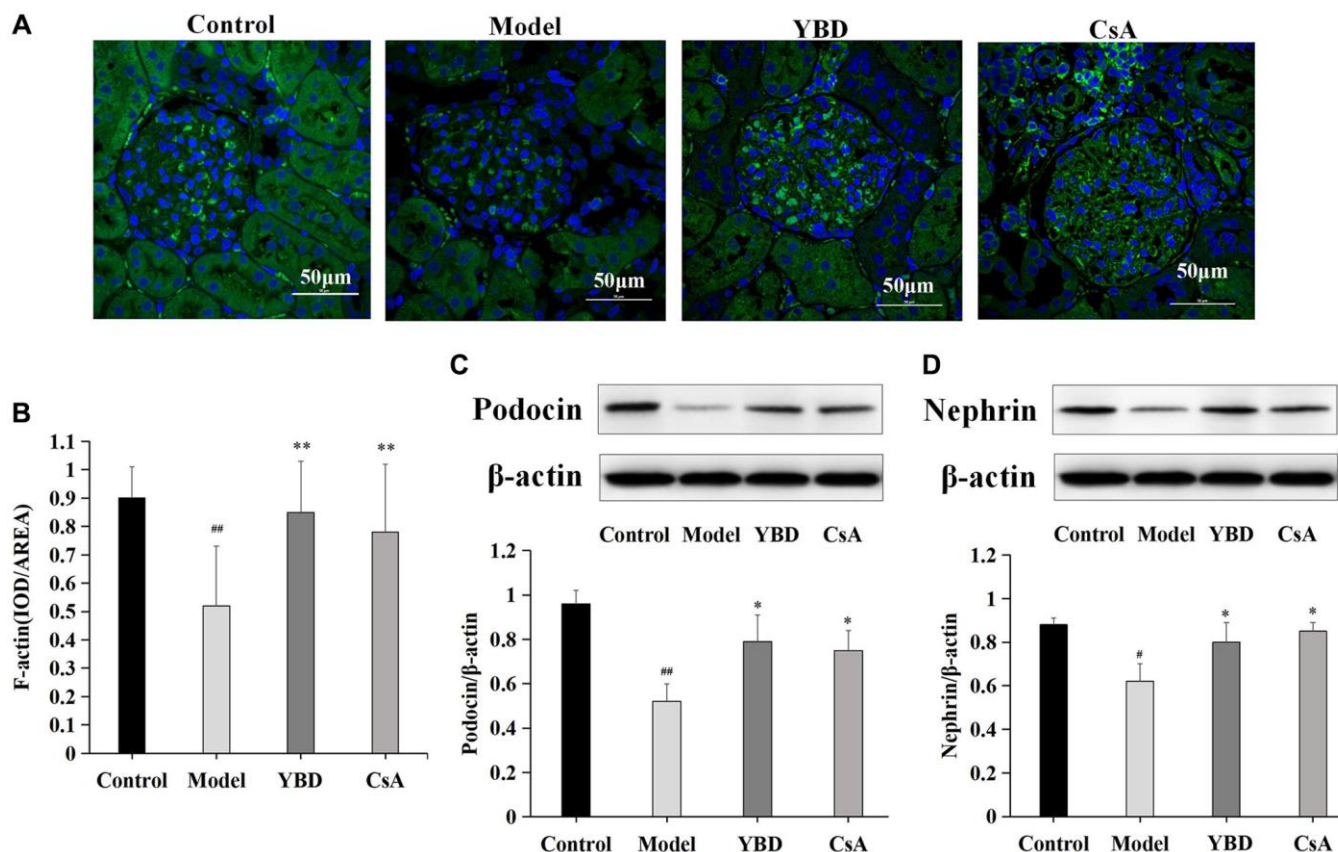
Figure 13. (**A**) F-actin in renal cortex tissues from different groups was shown by confocal microscopy (magnification × 600). Green staining showed positive expression of F-actin, and blue staining showed positive expression of cell nucleus. (**B**) The area of F-actin in different groups. (**C**, **D**) Western blotting analysis for the protein expression levels of podocin and nephrin in renal cortex tissues from different groups. As an internal control respectively, β-actin was used to calculate the quantification of protein. Data were expressed as mean ± SD, n = 6. Vertical bars represent the standard deviation. $^{\#}p < 0.05$ and $^{\#\#}p < 0.01$ versus control group; $^{*}p < 0.05$ and $^{**}p < 0.01$ versus model group.

PAN-induced NS model is a representative animal model and has been used to study glomerular proteinuria [65, 66]. When the model was successfully established, the massive proteinuria and decreased level of ALB was observed. Luckily, direct protective effects of YBD were observed in PAN-induced rats, including reducing proteinuria, decreasing blood pressure, increasing urine volume and ALB, ameliorating the condition of renal function and dyslipidemia. Through transmission electron microscopy, we found that the massive effacement and extensive fusion of podocyte foot processes were ameliorated with the treatment of YBD. Moreover, reduced expressions of nephrin and podocin, as well as actin-associated protein F-actin, were found in the NS rats, which were alleviated after administration of YBD. Although a previous study has shown that YBD can effectively regulate water metabolism to reduce lung and kidney edema of severe acute pancreatitis rats via decreasing aquaporins expression [67]. Our results provided the evidence that YBD protected against podocyte injury in PAN-induced NS rats through improving the expressions of nephrin, podocin and F-actin. In addition, western blotting analysis showed that YBD could significantly inhibit the expressions of PPP3CA, STAT3, NFATC3, TRPC6, and AKT1 in renal tissues. When combined with network pharmacology, it indicates YBD can been applied in treating NS by targeting proteins associated with podocyte injury, including PPP3CA, STAT3, NFATC3, TRPC6, and AKT1.

Obviously, these experiment results demonstrated the therapeutic effect of YBD, and verified the prediction information obtained through bioinformatics. However, it mainly focused on NS caused by podocyte injury. As is known, NS contains a variety of pathological types, including MCD, FSGS, MN, and IgAN [68]. Among them, MCD, FSGS, MN are characterized by different degrees of podocyte injury, which are known as the podocytopathy [69]. In this study, we examined effects of YBD on PAN-induced nephrosis rats, a well-established model of podocyte injury and human NS [70]. So, we speculated that YBD may be effective in treating certain pathological types of NS, such as MCD, FSGS, and MN.
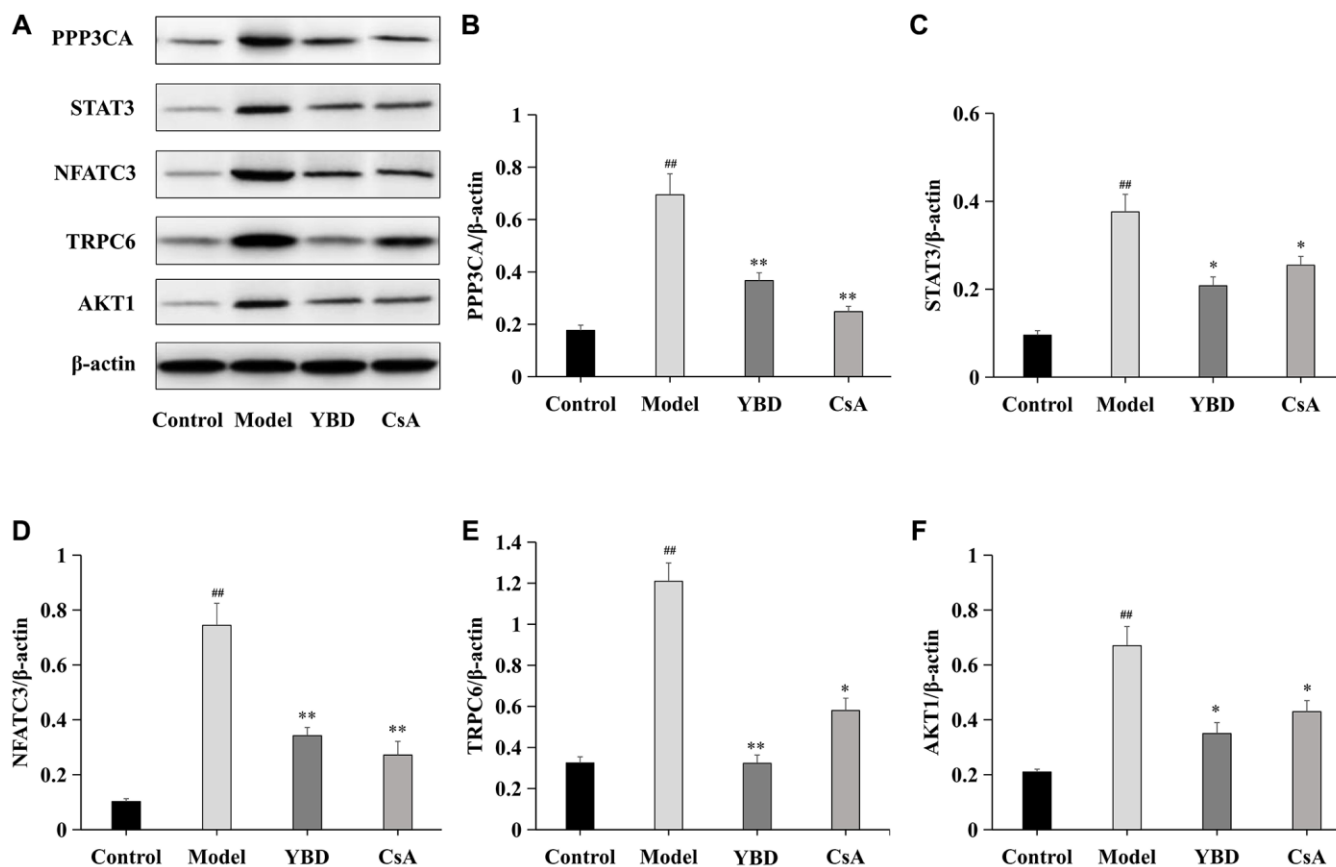
Figure 14. Effects of YBD on the expressions of core targets in NS rats induced by PAN. (**A–F**) The relative protein expressions of PPP3CA, STAT3, NFATC3, TRPC6, and AKT1 were measured by Western blotting. As an internal control respectively, β-actin was used to calculate the quantification of protein. Data were expressed as mean ± SD, n = 6. Vertical bars represent the standard deviation. $^{\#}p < 0.05$ and $^{\#\#}p < 0.01$ versus control group; $^{*}p < 0.05$ and $^{**}p < 0.01$ versus model group.

CONCLUSIONS

In summary, this study firstly puts forward a comprehensive strategy that combines bioinformatics and animal experiment to study material basis of YBD and its possible mechanisms against NS. Firstly, the relevant ingredients and core targets of YBD in treating NS were searched. Then, key ingredients, core targets (AKT1, STAT3, TRPC6, CASP3, JUN, PPP3CA, IL6, PTGS2, VEGFA, and NFATC3), and pathways related to podocyte injury (AGE-RAGE, and MAPK) were predicted by network pharmacology. Besides, molecular docking was applied to prove that ingredients had good affinity with target proteins. Finally, *in vivo* experiment confirmed effects of YBD and revealed that mechanisms are related to the regulations of PPP3CA, STAT3, NFATC3, TRPC6, and AKT1. However, the therapeutic effects and molecular mechanisms related to podocyte injury of YBD and its main active ingredients need to be studied in the future.

AUTHOR CONTRIBUTIONS

Tianwen Yao and Qingliang Wang designed the experiment and drafted the manuscript. Yi Wang contributed to the study design and gave the theoretical guidance. Shisheng Han performed the experiment and contributed to statistical analyses. Min Chen performed the experiment and helped to draft the manuscript. Yanqiu Xu was responsible for the revision of the final version. All authors read and approved the final manuscript.

CONFLICTS OF INTEREST

The authors declare no conflicts of interest related to this study.

ETHICAL STATEMENT

Animal welfare and experimental procedures were conducted in accordance with the principles of "Laboratory animal - Guidelines for ethical review of animal welfare (GB/T 35892-2018)", and approved by the Animal Ethics Committee of Yueyang Hospital of Integrated Traditional Chinese and Western Medicine affiliated to Shanghai University of Traditional Chinese Medicine (No. YYLAC-2019-016).

FUNDING

REFERENCES

1. Agrawal S, Zaritsky JJ, Fornoni A, Smoyer WE. Dyslipidaemia in nephrotic syndrome: mechanisms and treatment. Nat Rev Nephrol. 2018; 14:57–70.
https://doi.org/10.1038/nrneph.2017.155
PMID:29176657

2. Eckardt KU, Coresh J, Devuyst O, Johnson RJ, Köttgen A, Levey AS, Levin A. Evolving importance of kidney disease: from subspecialty to global health burden. Lancet. 2013; 382:158–69.
https://doi.org/10.1016/S0140-6736(13)60439-0
PMID:23727165

3. Veltkamp F, Rensma LR, Bouts AHM, and LEARNS consortium. Incidence and Relapse of Idiopathic Nephrotic Syndrome: Meta-analysis. Pediatrics. 2021; 148:e2020029249.
https://doi.org/10.1542/peds.2020-029249
PMID:34193618

4. Vivarelli M, Massella L, Ruggiero B, Emma F. Minimal Change Disease. Clin J Am Soc Nephrol. 2017; 12:332–45.
https://doi.org/10.2215/CJN.05000516
PMID:27940460

5. Kopp JB, Anders HJ, Susztak K, Podestà MA, Remuzzi G, Hildebrandt F, Romagnani P. Podocytopathies. Nat Rev Dis Primers. 2020; 6:68.
https://doi.org/10.1038/s41572-020-0196-7
PMID:32792490

6. Yu SM, Nissaisorakarn P, Husain I, Jim B. Proteinuric Kidney Diseases: A Podocyte's Slit Diaphragm and Cytoskeleton Approach. Front Med (Lausanne). 2018; 5:221.
https://doi.org/10.3389/fmed.2018.00221
PMID:30255020

7. Trautmann A, Schnaidt S, Lipska-Ziętkiewicz BS, Bodria M, Ozaltin F, Emma F, Anarat A, Melk A, Azocar M, Oh J, Saeed B, Gheisari A, Caliskan S, et al, and PodoNet Consortium. Long-Term Outcome of Steroid-Resistant Nephrotic Syndrome in Children. J Am Soc Nephrol. 2017; 28:3055–65.
https://doi.org/10.1681/ASN.2016101121
PMID:28566477

8. Lu H, Luo Y, Su B, Tang S, Chen G, Zhang L, Song C, Wang C, Tu H, Wu X. Wenyang Lishui Decoction Ameliorates Podocyte Injury in Membranous Nephropathy Rat and Cell Models by Regulating p53 and Bcl-2. Evid Based Complement Alternat Med. 2020; 2020:6813760.
https://doi.org/10.1155/2020/6813760
PMID:32454867

9. Cui FQ, Tang L, Gao YB, Wang YF, Meng Y, Shen C, Shen ZL, Liu ZQ, Zhao WJ, Liu WJ. Effect of

Baoshenfang Formula on Podocyte Injury via Inhibiting the NOX-4/ROS/p38 Pathway in Diabetic Nephropathy. J Diabetes Res. 2019; 2019:2981705.
https://doi.org/10.1155/2019/2981705
PMID:31179339

10. Yu ZK, Yang B, Zhang Y, Li LS, Zhao JN, Hao W. Modified Huangqi Chifeng decoction inhibits excessive autophagy to protect against Doxorubicin-induced nephrotic syndrome in rats via the PI3K/mTOR signaling pathway. Exp Ther Med. 2018; 16:2490–8.
https://doi.org/10.3892/etm.2018.6492
PMID:30210600

11. Han SS, Lu Y, Yao TW. The protective effects of Yue-bi-tang and Gu-jing-tang to PAN induced rats. J Tradit Chin Med. 2018; 51: 51–5.

12. Song CD, Song D, Jia PP. Effects of zhenwu decoction and yuebi decoction on AQP1/AQP2 in adriamycin nephropathy rats. Chinese Journal of Basic Medicine of Traditional Chinese Medicine. 2020; 26: 334–7.

13. Yan YJ. Clinical Observation on Modified Yuebi Decoction in the Treatment of Chronic Glomerulonephritis. Guangming Journal of Chinese Medicine. 2020; 37: 624–6.

14. Seif M, Deabes M, El-Askary A, El-Kott AF, Albadrani GM, Seif A, Wang Z. Ephedra sinica mitigates hepatic oxidative stress and inflammation via suppressing the TLR4/MyD88/NF-κB pathway in fipronil-treated rats. Environ Sci Pollut Res Int. 2021; 28:62943–58.
https://doi.org/10.1007/s11356-021-15142-4
PMID:34218381

15. Elhadef K, Smaoui S, Fourati M, Ben Hlima H, Chakchouk Mtibaa A, Sellem I, Ennouri K, Mellouli L. A Review on Worldwide *Ephedra* History and Story: From Fossils to Natural Products Mass Spectroscopy Characterization and Biopharmacotherapy Potential. Evid Based Complement Alternat Med. 2020; 2020:1540638.
https://doi.org/10.1155/2020/1540638
PMID:32419789

16. Luo CH, Ma LL, Liu HM, Liao W, Xu RC, Ci ZM, Lin JZ, Han L, Zhang DK. Research Progress on Main Symptoms of Novel Coronavirus Pneumonia Improved by Traditional Chinese Medicine. Front Pharmacol. 2020; 11:556885.
https://doi.org/10.3389/fphar.2020.556885
PMID:33013395

17. Ezzat SM, Ezzat MI, Okba MM, Menze ET, Abdel-Naim AB. The hidden mechanism beyond ginger (Zingiber officinale Rosc.) potent in vivo and in vitro anti-inflammatory activity. J Ethnopharmacol. 2018; 214:113–23.

https://doi.org/10.1016/j.jep.2017.12.019
PMID:29253614

18. Hua Y, Xu XX, Guo S, Xie H, Yan H, Ma XF, Niu Y, Duan JA. Wild Jujube (*Ziziphus jujuba* var. *spinosa*): A Review of Its Phytonutrients, Health Benefits, Metabolism, and Applications. J Agric Food Chem. 2022; 70:7871–86.
https://doi.org/10.1021/acs.jafc.2c01905
PMID:35731918

19. Jiang L, Shi Z, Yang Y. Network Pharmacology-Based Approach to Investigate the Molecular Targets of Rhubarb for Treating Cancer. Evid Based Complement Alternat Med. 2021; 2021:9945633.
https://doi.org/10.1155/2021/9945633
PMID:34211578

20. Zhang YC, Gao WC, Chen WJ, Pang DX, Mo DY, Yang M. Network Pharmacology and Molecular Docking Analysis on Molecular Targets and Mechanisms of Fei Jin Sheng Formula in the Treatment of Lung Cancer. Curr Pharm Des. 2023; 29:1121–34.
https://doi.org/10.2174/138161282966623050316475
5
PMID:37138492

21. Wang W, Li M, Si H, Jiang Z. Network Pharmacology and Integrated Molecular Docking Study on the Mechanism of the Therapeutic Effect of Fangfeng Decoction in Osteoarthritis. Curr Pharm Des. 2023; 29:379–92.
https://doi.org/10.2174/138161282966623021609565
9
PMID:36803762

22. Chen Y, Ma K, Si H, Duan Y, Zhai H. Network Pharmacology Integrated Molecular Docking to Reveal the Autism and Mechanism of Baohewan Heshiwei Wen Dan Tang. Curr Pharm Des. 2022; 28:3231–41.
https://doi.org/10.2174/138161282866622092609592
2
PMID:36165527

23. Liu J, Shi JL, Guo JY, Chen Y, Ma XJ, Wang SN, Zheng ZQ, Lin MX, He S. Anxiolytic-like effect of Suanzaoren-Wuweizi herb-pair and evidence for the involvement of the monoaminergic system in mice based on network pharmacology. BMC Complement Med Ther. 2023; 23:7.
https://doi.org/10.1186/s12906-022-03829-1
PMID:36624423

24. Doncheva NT, Morris JH, Gorodkin J, Jensen LJ. Cytoscape StringApp: Network Analysis and Visualization of Proteomics Data. J Proteome Res. 2019; 18:623–32.
https://doi.org/10.1021/acs.jproteome.8b00702
PMID:30450911

25. Guo Y, Li W, Cao Y, Feng X, Shen C, Gong S, Hou F, Yang Z, Chen X, Song J. Analysis of the potential biological mechanisms of Danyu Gukang Pill against osteonecrosis of the femoral head based on network pharmacology. BMC Complement Med Ther. 2023; 23:28. https://doi.org/10.1186/s12906-023-03843-x PMID:36721211

26. Yao T, Wang Q, Han S, Lu Y, Xu Y, Wang Y. Potential Molecular Mechanisms of Ephedra Herb in the Treatment of Nephrotic Syndrome Based on Network Pharmacology and Molecular Docking. Biomed Res Int. 2022; 2022:9214589. https://doi.org/10.1155/2022/9214589 PMID:35837376

27. Liu B, He Y, Lu R, Zhou J, Bai L, Zhang P, Ye S, Wu J, Liang C, Zhou Y, Zhou J. Zhen-wu-tang protects against podocyte injury in rats with IgA nephropathy via PPARγ/NF-κB pathway. Biomed Pharmacother. 2018; 101:635–47. https://doi.org/10.1016/j.biopha.2018.02.127 PMID:29518610

28. Tian R, Wang L, Chen A, Huang L, Liang X, Wang R, Mao W, Xu P, Bao K. Sanqi oral solution ameliorates renal damage and restores podocyte injury in experimental membranous nephropathy via suppression of NFκB. Biomed Pharmacother. 2019; 115:108904. https://doi.org/10.1016/j.biopha.2019.108904 PMID:31060008

29. Kho MC, Park JH, Han BH, Tan R, Yoon JJ, Kim HY, Ahn YM, Lee YJ, Kang DG, Lee HS. Plantago asiatica L. Ameliorates Puromycin Aminonucleoside-Induced Nephrotic Syndrome by Suppressing Inflammation and Apoptosis. Nutrients. 2017; 9:386. https://doi.org/10.3390/nu9040386 PMID:28420111

30. Shen X, Jiang H, Ying M, Xie Z, Li X, Wang H, Zhao J, Lin C, Wang Y, Feng S, Shen J, Weng C, Lin W, et al. Calcineurin inhibitors cyclosporin A and tacrolimus protect against podocyte injury induced by puromycin aminonucleoside in rodent models. Sci Rep. 2016; 6:32087. https://doi.org/10.1038/srep32087 PMID:27580845

31. Li C, Zhu F, Wang S, Wang J, Wu B. Danggui Buxue Decoction Ameliorates Inflammatory Bowel Disease by Improving Inflammation and Rebuilding Intestinal Mucosal Barrier. Evid Based Complement Alternat Med. 2021; 2021:8853141. https://doi.org/10.1155/2021/8853141 PMID:33531923

32. Jiang L, Cui H, Ding J, Yang A, Zhang Y. Puromycin aminonucleoside-induced podocyte injury is ameliorated by the Smad3 inhibitor SIS3. FEBS Open Bio. 2020; 10:1601–11. https://doi.org/10.1002/2211-5463.12916 PMID:32583562

33. Gao W, Liu Y, Fan L, Zheng B, Jefferson JR, Wang S, Zhang H, Fang X, Nguyen BV, Zhu T, Roman RJ, Fan F. Role of γ-adducin in actin cytoskeleton rearrangements in podocyte pathophysiology. Am J Physiol Renal Physiol. 2021; 320:F97–113. https://doi.org/10.1152/ajprenal.00423.2020 PMID:33308016

34. Baijnath S, Murugesan S, Mackraj I, Gathiram P, Moodley J. The effects of sildenafil citrate on urinary podocin and nephrin mRNA expression in an L-NAME model of pre-eclampsia. Mol Cell Biochem. 2017; 427:59–67. https://doi.org/10.1007/s11010-016-2897-5 PMID:27995418

35. Qi XM, Wang J, Xu XX, Li YY, Wu YG. FK506 reduces albuminuria through improving podocyte nephrin and podocin expression in diabetic rats. Inflamm Res. 2016; 65:103–14. https://doi.org/10.1007/s00011-015-0893-y PMID:26566632

36. Ahn W, Bomback AS. Approach to Diagnosis and Management of Primary Glomerular Diseases Due to Podocytopathies in Adults: Core Curriculum 2020. Am J Kidney Dis. 2020; 75:955–64. https://doi.org/10.1053/j.ajkd.2019.12.019 PMID:32331832

37. Yoshimura Y, Nishinakamura R. Podocyte development, disease, and stem cell research. Kidney Int. 2019; 96:1077–82. https://doi.org/10.1016/j.kint.2019.04.044 PMID:31420196

38. Verma R, Venkatareddy M, Kalinowski A, Li T, Kukla J, Mollin A, Cara-Fuentes G, Patel SR, Garg P. Nephrin is necessary for podocyte recovery following injury in an adult mature glomerulus. PLoS One. 2018; 13:e0198013. https://doi.org/10.1371/journal.pone.0198013 PMID:29924795

39. Sang Y, Tsuji K, Inoue-Torii A, Fukushima K, Kitamura S, Wada J. Semaphorin3A-Inhibitor Ameliorates Doxorubicin-Induced Podocyte Injury. Int J Mol Sci. 2020; 21:4099. https://doi.org/10.3390/ijms21114099 PMID:32521824

40. Maier JI, Rogg M, Helmstädter M, Sammarco A, Walz G, Werner M, Schell C. A Novel Model for Nephrotic Syndrome Reveals Associated Dysbiosis of the Gut Microbiome and Extramedullary Hematopoiesis. Cells. 2021; 10:1509.

https://doi.org/10.3390/cells10061509
PMID:34203913

41. Wang S, Ji T, Wang L, Qu Y, Wang X, Wang W, Lv M, Wang Y, Li X, Jiang P. Exploration of the mechanism by which Huangqi Guizhi Wuwu decoction inhibits Lps-induced inflammation by regulating macrophage polarization based on network pharmacology. BMC Complement Med Ther. 2023; 23:8.
https://doi.org/10.1186/s12906-022-03826-4
PMID:36624435

42. Pilařová V, Kuda L, Vlčková HK, Nováková L, Gupta S, Kulkarni M, Švec F, Van Staden J, Doležal K. Carbon dioxide expanded liquid: an effective solvent for the extraction of quercetin from South African medicinal plants. Plant Methods. 2022; 18:87.
https://doi.org/10.1186/s13007-022-00919-6
PMID:35739596

43. Liu Y, Li Y, Xu L, Shi J, Yu X, Wang X, Li X, Jiang H, Yang T, Yin X, Du L, Lu Q. Quercetin Attenuates Podocyte Apoptosis of Diabetic Nephropathy Through Targeting EGFR Signaling. Front Pharmacol. 2022; 12:792777.
https://doi.org/10.3389/fphar.2021.792777
PMID:35069207

44. Xiao X, Hu Q, Deng X, Shi K, Zhang W, Jiang Y, Ma X, Zeng J, Wang X. Old wine in new bottles: Kaempferol is a promising agent for treating the trilogy of liver diseases. Pharmacol Res. 2022; 175:106005.
https://doi.org/10.1016/j.phrs.2021.106005
PMID:34843960

45. Li Y, Zheng D, Shen D, Zhang X, Zhao X, Liao H. Protective Effects of Two Safflower Derived Compounds, Kaempferol and Hydroxysafflor Yellow A, on Hyperglycaemic Stress-Induced Podocyte Apoptosis via Modulating of Macrophage M1/M2 Polarization. J Immunol Res. 2020; 2020:2462039.
https://doi.org/10.1155/2020/2462039
PMID:33102606

46. Xu H, Yu W, Sun S, Li C, Zhang Y, Ren J. Luteolin Attenuates Doxorubicin-Induced Cardiotoxicity Through Promoting Mitochondrial Autophagy. Front Physiol. 2020; 11:113.
https://doi.org/10.3389/fphys.2020.00113
PMID:32116805

47. Tang L, Deng B, Shi L, Wei B, Ren B, Fu X. Effect of Luteolin on 11Beta-Hydroxysteroid Dehydrogenase in Rat Liver and Kidney. Evid Based Complement Alternat Med. 2015; 2015:834124.
https://doi.org/10.1155/2015/834124
PMID:26199637

48. Yu Q, Zhang M, Qian L, Wen D, Wu G. Luteolin attenuates high glucose-induced podocyte injury via suppressing NLRP3 inflammasome pathway. Life Sci. 2019; 225:1–7.
https://doi.org/10.1016/j.lfs.2019.03.073
PMID:30935950

49. Yao T, Su W, Han S, Lu Y, Xu Y, Chen M, Wang Y. Recent Advances in Traditional Chinese Medicine for Treatment of Podocyte Injury. Front Pharmacol. 2022; 13:816025.
https://doi.org/10.3389/fphar.2022.816025
PMID:35281899

50. Hall G, Wang L, Spurney RF. TRPC Channels in Proteinuric Kidney Diseases. Cells. 2019; 9:44.
https://doi.org/10.3390/cells9010044
PMID:31877991

51. Huang H, You Y, Lin X, Tang C, Gu X, Huang M, Qin Y, Tan J, Huang F. Inhibition of TRPC6 Signal Pathway Alleviates Podocyte Injury Induced by TGF-β1. Cell Physiol Biochem. 2017; 41:163–72.
https://doi.org/10.1159/000455985
PMID:28214865

52. Kim EY, Yazdizadeh Shotorbani P, Dryer SE. Trpc6 inactivation confers protection in a model of severe nephrosis in rats. J Mol Med (Berl). 2018; 96:631–44.
https://doi.org/10.1007/s00109-018-1648-3
PMID:29785489

53. Polat OK, Uno M, Maruyama T, Tran HN, Imamura K, Wong CF, Sakaguchi R, Ariyoshi M, Itsuki K, Ichikawa J, Morii T, Shirakawa M, Inoue R, et al. Contribution of Coiled-Coil Assembly to Ca^{2+}/Calmodulin-Dependent Inactivation of TRPC6 Channel and its Impacts on FSGS-Associated Phenotypes. J Am Soc Nephrol. 2019; 30:1587–603.
https://doi.org/10.1681/ASN.2018070756
PMID:31266820

54. Karagiota A, Mylonis I, Simos G, Chachami G. Protein phosphatase PPP3CA (calcineurin A) down-regulates hypoxia-inducible factor transcriptional activity. Arch Biochem Biophys. 2019; 664:174–82.
https://doi.org/10.1016/j.abb.2019.02.007
PMID:30776328

55. Ma R, Xu Y, Zhou H, Zhang D, Yao D, Song L, Liu Y. Participation of the AngII/TRPC6/NFAT axis in the pathogenesis of podocyte injury in rats with type 2 diabetes. Mol Med Rep. 2019; 19:2421–30.
https://doi.org/10.3892/mmr.2019.9871
PMID:30664212

56. Kawachi H, Fukusumi Y. New insight into podocyte slit diaphragm, a therapeutic target of proteinuria. Clin Exp Nephrol. 2020; 24:193–204.
https://doi.org/10.1007/s10157-020-01854-3
PMID:32020343

57. Golus M, Bugajski P, Chorbińska J, Krajewski W, Lemiński A, Saczko J, Kulbacka J, Szydełko T, Małkiewicz B. STAT3 and Its Pathways' Dysregulation-Underestimated Role in Urological Tumors. Cells. 2022; 11:3024.
https://doi.org/10.3390/cells11193024
PMID:36230984

58. Zhou J, Yang J, Wang YM, Ding H, Li TS, Liu ZH, Chen L, Jiao RQ, Zhang DM, Kong LD. IL-6/STAT3 signaling activation exacerbates high fructose-induced podocyte hypertrophy by ketohexokinase-A-mediated tristetraprolin down-regulation. Cell Signal. 2021; 86:110082.
https://doi.org/10.1016/j.cellsig.2021.110082
PMID:34252535

59. Ma X, Hao C, Yu M, Zhang Z, Huang J, Yang W. Investigating the Molecular Mechanism of Quercetin Protecting against Podocyte Injury to Attenuate Diabetic Nephropathy through Network Pharmacology, MicroarrayData Analysis, and Molecular Docking. Evid Based Complement Alternat Med. 2022; 2022:7291434.
https://doi.org/10.1155/2022/7291434
PMID:35615688

60. Inoue K, Ishibe S. Podocyte endocytosis in the regulation of the glomerular filtration barrier. Am J Physiol Renal Physiol. 2015; 309:F398–405.
https://doi.org/10.1152/ajprenal.00136.2015
PMID:26084928

61. Afsar B, Afsar RE, Demiray A, Covic A, Kanbay M. Deciphering nutritional interventions for podocyte structure and function. Pharmacol Res. 2021; 172:105852.
https://doi.org/10.1016/j.phrs.2021.105852
PMID:34450318

62. Pathomthongtaweechai N, Chutipongtanate S. AGE/RAGE signaling-mediated endoplasmic reticulum stress and future prospects in non-coding RNA therapeutics for diabetic nephropathy. Biomed Pharmacother. 2020; 131:110655.
https://doi.org/10.1016/j.biopha.2020.110655
PMID:32853909

63. Long C, Lin Q, Mo J, Xiao Y, Xie Y. Hirudin attenuates puromycin aminonucleoside-induced glomerular podocyte injury by inhibiting MAPK-mediated endoplasmic reticulum stress. Drug Dev Res. 2022; 83:1047–56.
https://doi.org/10.1002/ddr.21932
PMID:35277865

64. Yuan C, Wang MH, Wang F, Chen PY, Ke XG, Yu B, Yang YF, You PT, Wu HZ. Network pharmacology and molecular docking reveal the mechanism of Scopoletin against non-small cell lung cancer. Life Sci. 2021; 270:119105.
https://doi.org/10.1016/j.lfs.2021.119105
PMID:33497736

65. Jo CH, Kim S, Kim GH. Association of Proteinuria with Urinary Concentration Defect in Puromycin Aminonucleoside Nephrosis. Electrolyte Blood Press. 2020; 18:31–9.
https://doi.org/10.5049/EBP.2020.18.2.31
PMID:33408745

66. Shen X, Zhang Y, Lin C, Weng C, Wang Y, Feng S, Wang C, Shao X, Lin W, Li B, Wang H, Chen J, Jiang H. Calcineurin inhibitors ameliorate PAN-induced podocyte injury through the NFAT-Angptl4 pathway. J Pathol. 2020; 252:227–38.
https://doi.org/10.1002/path.5512
PMID:32686149

67. Hu J, Zhang YM, Miao YF, Zhu L, Yi XL, Chen H, Yang XJ, Wan MH, Tang WF. Effects of Yue-Bi-Tang on water metabolism in severe acute pancreatitis rats with acute lung-kidney injury. World J Gastroenterol. 2020; 26:6810–21.
https://doi.org/10.3748/wjg.v26.i43.6810
PMID:33268963

68. Chebotareva N, Vinogradov A, Cao V, Gindis A, Berns A, Alentov I, Sergeeva N. Serum levels of plasminogen activator urokinase receptor and cardiotrophin-like cytokine factor 1 in patients with nephrotic syndrome. Clin Nephrol. 2022; 97:103–10.
https://doi.org/10.5414/CN110514
PMID:34779387

69. Müller-Deile J, Schenk H, Schiffer M. Minimal-change-Glomerulonephritis und fokal-segmentale Glomerulosklerose [Minimal change disease and focal segmental glomerulosclerosis]. Internist (Berl). 2019; 60:450–7.
https://doi.org/10.1007/s00108-019-0590-y
PMID:30887070

70. Xiao M, Bohnert BN, Grahammer F, Artunc F. Rodent models to study sodium retention in experimental nephrotic syndrome. Acta Physiol (Oxf). 2022; 235:e13844.
https://doi.org/10.1111/apha.13844
PMID:35569011

SUPPLEMENTARY MATERIALS

Please browse Full Text version to see the data of Supplementary Table 4.

Supplementary Tables

Supplementary Table 1. A total of 124 different active ingredients from TCMSP and literature in YBD.

Ingredients	Herb	Symbol
(+)-Catechin	MH	A1
(+)-Leucocyanidin	MH	MH1
24-Ethylcholest-4-en-3-one	MH	MH2
Beta-sitosterol	MH	B1
Campest-5-en-3beta-ol	MH	MH3
Delphinidin	MH	MH4
Diosmetin	MH	MH5
Eriodictyol	MH	MH6
Genkwanin	MH	MH7
Herbacetin	MH	MH8
Kaempferol	MH	E1
Leucopelargonidin	MH	MH9
Luteolin	MH	MH10
Mandenol	MH	MH11
Naringenin	MH	E2
Pectolinarigenin	MH	MH12
Poriferast-5-en-3beta-ol	MH	D1
Quercetin	MH	C1
Resivit	MH	MH13
Stigmasterol	MH	B2
Taxifolin	MH	MH14
Truflex OBP	MH	MH15
stepharine	DZ	DZ1
zizyphus saponin I_qt	DZ	DZ2
coumestrol	DZ	DZ3
Daechuine S7	DZ	DZ4
Jujubasaponin V_qt	DZ	DZ5
Mauritine D	DZ	DZ6
berberine	DZ	DZ7
(S)-Coclaurine	DZ	DZ8
Mairin	DZ	F1
Stigmasterol	DZ	B2
beta-sitosterol	DZ	B1
Ruvoside_qt	DZ	DZ9
(+)-catechin	DZ	A1
Stepholidine	DZ	DZ10
Nuciferin	DZ	DZ11
Fumarine	DZ	DZ12
beta-carotene	DZ	DZ13
(−)-catechin	DZ	DZ14
quercetin	DZ	C1

beta-sitosterol	SJ	B1
6-methylgingediacetate2	SJ	SJ1
Stigmasterol	SJ	B2
poriferast-5-en-3beta-ol	SJ	D1
Dihydrocapsaicin	SJ	SJ2
CaSO4	SG	SG
quercetin	GC	C1
Mairin	GC	F1
Jaranol	GC	GC1
isorhamnetin	GC	GC2
sitosterol	GC	GC3
formononetin	GC	GC4
Calycosin	GC	GC5
kaempferol	GC	GC6
licochalcone a	GC	E1
Vestitol	GC	GC7
Inermine	GC	GC8
DFV	GC	GC9
Glycyrol	GC	GC10
Medicarpin	GC	GC11
Lupiwighteone	GC	GC12
7-Methoxy-2-methyl isoflavone	GC	GC13
naringenin	GC	GC14
(2S)-2-[4-hydroxy-3-(3-methylbut-2-enyl)phenyl]-8,8-dimethyl-2,3-dihydropyrano[2,3-f]chromen-4-one	GC	E2
euchrenone	GC	GC15
glyasperin B	GC	GC16
glyasperin F	GC	GC17
Glyasperin C	GC	GC18
Isotrifoliol	GC	GC19
(E)-1-(2,4-dihydroxyphenyl)-3-(2,2-dimethylchromen-6-yl)prop-2-en-1-one	GC	GC20
kanzonols W	GC	GC21
(2S)-6-(2,4-dihydroxyphenyl)-2-(2-hydroxypropan-2-yl)-4-methoxy-2,3-dihydrofuro[3,2-g]chromen-7-one	GC	GC22
Semilicoisoflavone B	GC	GC23
Glepidotin A	GC	GC24
Glepidotin B	GC	GC25
Phaseolinisoflavan	GC	GC26
Glypallichalcone	GC	GC27
8-(6-hydroxy-2-benzofuranyl)-2,2-dimethyl-5-chromenol	GC	GC28
Licochalcone B	GC	GC29
licochalcone G	GC	GC30
3-(2,4-dihydroxyphenyl)-8-(1,1-dimethylprop-2-enyl)-7-hydroxy-5-methoxy-coumarin	GC	GC31
Licoricone	GC	GC32
Gancaonin A	GC	GC33
Gancaonin B	GC	GC34
3-(3,4-dihydroxyphenyl)-5,7-dihydroxy-8-(3-methylbut-2-enyl)chromone	GC	GC35
5,7-dihydroxy-3-(4-methoxyphenyl)-8-(3-methylbut-2-enyl)chromone	GC	GC36
2-(3,4-dihydroxyphenyl)-5,7-dihydroxy-6-(3-methylbut-2-enyl)chromone	GC	GC37
Glycyrin	GC	GC38

Licocoumarone	GC	GC39
Licoisoflavone	GC	GC40
Licoisoflavone B	GC	GC41
licoisoflavanone	GC	GC42
shinpterocarpin	GC	GC43
(E)-3-[3,4-dihydroxy-5-(3-methylbut-2-enyl)phenyl]-1-(2,4-dihydroxyphenyl)prop-2-en-1-one	GC	GC44
liquiritin	GC	GC45
licopyranocoumarin	GC	GC46
Glyzaglabrin	GC	GC47
Glabridin	GC	GC48
Glabranin	GC	GC49
Glabrene	GC	GC50
Glabrone	GC	GC51
1,3-dihydroxy-9-methoxy-6-benzofurano[3,2-c]chromenone	GC	GC52
1,3-dihydroxy-8,9-dimethoxy-6-benzofurano[3,2-c]chromenone	GC	GC53
Eurycarpin A	GC	GC54
(−)-Medicocarpin	GC	GC55
Sigmoidin-B	GC	GC56
(2R)-7-hydroxy-2-(4-hydroxyphenyl)chroman-4-one	GC	GC57
(2S)-7-hydroxy-2-(4-hydroxyphenyl)-8-(3-methylbut-2-enyl)chroman-4-one	GC	GC58
Isoglycyrol	GC	GC59
Isolicoflavonol	GC	GC60
HMO	GC	GC61
1-Methoxyphaseollidin	GC	GC62
Quercetin der.	GC	GC63
3'-Hydroxy-4'-O-Methylglabridin	GC	GC64
3'-Methoxyglabridin	GC	GC65
2-[(3R)-8,8-dimethyl-3,4-dihydro-2H-pyrano[6,5-f]chromen-3-yl]-5-methoxyphenol	GC	GC66
Inflacoumarin A	GC	GC67
icos-5-enoic acid	GC	GC68
Kanzonol F	GC	GC69
6-prenylated eriodictyol	GC	GC70
7,2',4'-trihydroxy-5-methoxy-3-arylcoumarin	GC	GC71
7-Acetoxy-2-methylisoflavone	GC	GC72
8-prenylated eriodictyol	GC	GC73
gadelaidic acid	GC	GC74
Gancaonin G	GC	GC75
Gancaonin H	GC	GC76
Licoagrocarpin	GC	GC77
Glyasperins M	GC	GC78
Glycyrrhiza flavonol A	GC	GC79
Licoagroisoflavone	GC	GC80
Odoratin	GC	GC81
Phaseol	GC	GC82
Xambioona	GC	GC83
dehydroglyasperins C	GC	GC84

Supplementary Table 2. Targets information of different ingredients in YBD through SwissTargetPrediction and TCMSP.

PSMD3	target	HSPB1	target	RAF1	target	GABRA2	target	CHRNA7	target
MMP2	target	HMOX1	target	RASSF1	target	IKBKB	target	CHRNA2	target
HSPA5	target	HK2	target	RASA1	target	MAPK8	target	JUN	target
ACHE	target	NKX3-1	target	ERBB2	target	CHRM2	target	TGFB1	target
ACACA	target	HAS2	target	ERBB3	target	SLC6A2	target	F10	target
AHSA1	target	HIF1A	target	RB1	target	CA2	target	ADH1C	target
AKR1B1	target	CHUK	target	RXRA	target	CDK4	target	ADRA2A	target
MAOB	target	INSR	target	RUNX2	target	FOSL2	target	MAOA	target
AR	target	IGF2	target	CHEK2	target	STAT3	target	CTRB1	target
BAX	target	IGFBP3	target	PON1	target	HTR2A	target	DRD5	target
BCL2	target	ICAM1	target	STAT1	target	CHRM4	target	ADRA2B	target
ALOX5	target	IFNG	target	SCN5A	target	HTR3A	target	DRD2	target
AHR	target	IRF1	target	SLC2A4	target	ADRA1D	target	CYP2B6	target
BIRC5	target	IL1A	target	MMP3	target	IGHG1	target	CDC37	target
BCL2L1	target	IL1B	target	SOD1	target	CHRM3	target	PDE10A	target
ADRB2	target	IL10	target	THBD	target	OPRM1	target	ADRA2C	target
CASP3	target	IL2	target	F3	target	KDR	target	LACTB	target
CASP8	target	IL6	target	PLAT	target	OPRD1	target	DRD4	target
CASP9	target	CXCL8	target	E2F1	target	DRD1	target	HTR2C	target
CTSD	target	MMP1	target	E2F2	target	MAPK10	target	TOP2	target
CAV1	target	MMP9	target	RELA	target	CHRM5	target	PDE4	target
CCL2	target	MAPK1	target	PRSS1	target	ADRB1	target	CACNA1S	target
CD40LG	target	MYC	target	NFATC3	target	LTA4H	target	CYP2B1	target
TP53	target	MPO	target	DIO1	target	HMGCR	target	ALB	target
CLDN4	target	NQO1	target	PLAU	target	ABAT	target	CTNNB1	target
F7	target	POR	target	VCAM1	target	ADIPOQ	target	CASP7	target
COL1A1	target	NCF1	target	VEGFA	target	AKR1C1	target	MMP10	target
COL3A1	target	NFKBIA	target	PPP3CA	target	APOB	target	KLF7	target
CRP	target	NOS3	target	PGR	target	GOT1	target	GRP78	target
CXCL10	target	NFE2L2	target	CDK2	target	BAD	target	ABCG2	target
CXCL11	target	NCOA2	target	ESR2	target	CAT	target	CDC2	target
CXCL2	target	NR1I2	target	NOS2	target	CYP19A1	target	CDKN2A	target
CDKN1A	target	NR1I3	target	CHEK1	target	FASN	target	IL8	target
CYP1A1	target	ODC1	target	CCNA2	target	GSR	target	MGAM	target
CYP1A2	target	SPP1	target	ESR1	target	CES1	target	HERC5	target
CYP1B1	target	PPARG	target	GRIA2	target	LDLR	target	F2	target
CYP3A4	target	PPARA	target	PYGM	target	MTTP	target	PPP3CB	target
DCAF5	target	PPARD	target	GSK3B	target	MAPK3	target	ADCY2	target
DPP4	target	PTEN	target	MAPK14	target	ABCC1	target	APP	target
TOP1	target	PIK3CG	target	NCOA1	target	PLB1	target	XIAP	target
TOP2A	target	SERPINE1	target	OLR1	target	SOAT1	target	MDM2	target
DUOX2	target	PARP1	target	NR3C2	target	SOAT2	target	MET	target
EGFR	target	KCNH2	target	HSD3B1	target	SREBF1	target	MCL1	target
SELE	target	PCOLCE	target	HSD3B2	target	UGT1A1	target	NUF2	target
SULT1E1	target	EGF	target	ADRA1A	target	RXRB	target	PCNA	target
ELK1	target	PTGER3	target	ATP5F1B	target	KCNMA1	target	PTGES	target
EIF6	target	PTGS1	target	PKIA	target	TFRC	target	TYR	target
CCND1	target	PTGS2	target	IL4	target	FN1	target	XDH	target
CCNB1	target	ACP3	target	CHRM1	target	TRPC6	target	DGAT2	target
GABRA1	target	RUNX1T1	target	MT-ND6	target	PDE3A	target		
GJA1	target	PRKCA	target	SLC6A3	target	GABRA3	target		
GSTM1	target	PRKCB	target	SLC6A4	target	GABRA5	target		

GSTM2	target	FOS	target	AKR1C3	target	HSP90	target
GSTP1	target	NPEPPS	target	ADRA1B	target	MAP2	target
HSF1	target	AKT1	target	SLPI	target	PRKACA	target

Supplementary Table 3. Overlapping targets information of drug targets and disease targets.

MMP2
XDH
HSPB1
NOS2
COL1A1
PPP3CA
BCL2
CRP
GSTP1
FN1
EGF
IL1A
LDLR
SPP1
F2
XIAP
PTGS2
OLR1
CTNNB1
CCND1
CDK4
NFATC3
VEGFA
TGFB1
MYC
CCNA2
MT-ND6
MMP1
STAT1
HMGCR
NR3C2
GSR
HMOX1
MMP3
PPP3CB
GSTM1
IL10
MAPK1
PLAT
MDM2
EGFR
SOD1
ERBB2
IL4
AKR1B1
TRPC6
IGHG1
RUNX2
CXCL10
TP53
CASP9
CDKN1A
CAT
RASA1

IL1B
NFKBIA
IGFBP3
ALB
SLC6A3
LTA4H
PLAU
PTEN
ALOX5
RXRA
CLDN4
PON1
E2F1
APOB
CASP8
PPARG
CXCL8
SELE
THBD
MAPK14
MPO
PCNA
CHUK
STAT3
SLPI
ADRB2
CTSD
TFRC
MCL1
CCL2
IL6
CASP3
PARP1
MGAM
KDR
IGF2
PIK3CG
IL2
IFNG
FOS
HSPA5
ICAM1
BCL2L1
MAPK3
HIF1A
RELA
NOS3
SERPINE1
VCAM1
INSR
AKT1
PTGS1
F3
PYGM
CDKN2A
JUN
BAX
PRKCA
CD40LG
CYP3A4
SCN5A

APP
MMP9
TOP1
ADIPOQ

Supplementary Table 4. Detailed information on GO enrichment analysis.

Supplementary Table 5. Detail information on the known ligands of the top five targets.

Target	Known ligand	Full name of ligand	Molecular weight	Molecular formula	Affinity energy (kcal/mol)
AKT1	UC8	~{N}-methyl-6-[4-[[4-[2-oxidanylidene-6- (propanoylamino)-3~{H}-benzimidazol-1- yl]piperidin-1-yl]methyl]phenyl]-5-phenyl- pyridine-3-carboxamide	588.7	C35H36N6O3	−6.2
TRPC6	POV	(2S)-3-(hexadecanoyloxy)-2- [(9Z)-octadec-9- enoyloxy]propyl 2-(trimethylammonio)ethyl phosphate	760.08	C42H82NO8P	−8.0
STAT3	KQV	[(2-{[[(5S,8S,10aR)-3-acetyl-8-({(2S)-5-amino-1-[(diphenylmethyl)amino]- 1,5-dioxopentan-2- yl}carbamoyl)-6-oxodecahydropyrrolo[1,2-a][1,5]diazocin-5- yl]carbamoyl}-1H-indol-5- yl)(difluoro)methyl]phosph onic acid (non-preferred name)	835.79	40H44F2N7O9	−7.1
PPP3CA	PGE	TRIETHYLENE GLYCOL	150.17	C6H14O4	−7.8
NFATC	3ANP	PHOSPHOAMINOPHOSP HONIC ACID-ADENYLATE ESTER	506.2	10H17N6O12P	−8.2